UNIVERSIDADE DE LISBOA
FACULDADE DE CIÊNCIAS
DEPARTAMENTO DE QUÍMICA E BIOQUÍMICA

Cellulose Liquefaction: Optimization of Reaction Parameters

Filipe Manuel Castelhano Figueiredo

Mestrado em Química Tecnológica

Dissertação orientada por:

Doutora Ana Filipa Russo de Albuquerque Cristino Doutora Maria

Margarida Pires dos Santos Mateus

2021

Acknowledgments

First of all I want to thank my advisors Dtr. Ana Cristino and Dtr. Margarida Mateus for all the guidance and efforts to help me perform the best possible work. Withoout them, this would have been a much harder path. This honors also apply for Dtr Rui Galhano dos Santos who I also am thankful for all the help.

I want to thank Professor Maria José Lourenço and all the professors for believing in me and helping me throughout both the bachelor and the masters degree.

I also want to thank the help provided in and off the laboratory from Mário Vale, David Duarte, Miguel Monteiro, Professor José Condeço and Dtr. Xavier Paredes.

I want to give a special thank you note to my parents for always sticking by my side and for always believing in me. This would never had been possible without them.

Atlast, thank you to all my friends who I can't write all names but they know who they are.

I. Resumo

Neste trabalho estudou-se a optimização dos parâmetros reacionais da liquefação direta de biomassa lignocelulósica. O solvente usado foi 2-etilhexanol com um liquor ratio de 5:1 (solvente:biomassa), juntamente com o catalisador ácido p-toluenossulfónico (PTSA). Com o objectivo de obter a defnir um modelo experimental, foram efectuadas 17 reacções variando parâmetros como a temperatura, o tempo de reacção e a quantidade de catalisador. As condições ideais foram obtidas a 170 ºC, com 3 horas de reacção e 3% (m/m) de catalisador, resultando num rendimento de 84.8%.

Os bio-óleos produzidos foram caracterizados por espectroscopia de infravermelhos e análise elementar tendo-se também determinado a densidade e as viscosidades cinemática e dinâmica.

A avaliação dos resultados permitiu confirmar que a temperatura se trata do parâmetro reacional mais influente tendo-se concluído que abaixo dos 170 ºC não se verifica a formação de um grupo carbonilo no espectro FTIR do bio-óleo. O aumento de reacções secundárias com o aumento do tempo de reação também é verificado pela espectroscopia de infravermelhos. As propriedades químicas dos bio-óleos, como a densidade e ambos os tipos de viscosidade, aumentam com a conversão da celulose.

A análise elementar permitiu estimar o HHV dos bio-óleos e dos resíduos sólidos tendo sido 30.16 MJ Kg^{-1} o maior valor obtido, um valor ainda distante dos derivados de combustíveis fósseis. No entanto, o HHV dos resíduos sólidos revelou-se superior ao da celulose pura potenciando a hipótese de aplicar o processo de liquefação ao resíduo sólido de liquefações posteriores.

Palavras-chave: liquefação, biomassa, bio-óleo, variáveis operatórias

II. Abstract

The present work studied the optimization of the reaction parameters in lignocellulosic biomass liquefaction. The solvent used was 2-ethylhexanol with a 5:1 liquor ratio (solvent:biomass) and the used catalyst was p-toluenosulfonic acid (PTSA). To understand the best reaction media for the biomass conversion, 17 reactions were performed varying the reaction temperature, reaction time and catalyst amount. The optimum conditions were 170 ºC, 3 hours and 3 wt%(m/m) of catalyst which produced the highest reported yield – 84.8%.

The produced bio-oils were characterized by infrared spectroscopy and elementar analysis with the densities and viscosities, both kinematic and dynamic, also determined.

The evaluation of the results confirmed that temperature is the most influential reactional parameter with the FTIR results showing that under 170 ºC no carbonyl groups are formed. The infrared spectroscopy also confirms the increase of secondary reactions with the longer reaction times. Density and viscosity values increased with the conversion of cellulose.

The elementar analysis allowed to estimate the high heating value of the bio-oils and solid-residues with the highest bio-oil HHV achieved being 30.16 MJ Kg^{-1}, a distant value from the ones derived from fossil fuels. Although, the solid-residues HHV were superior to pure cellulose's HHV potentiating the hypothesis of reusing the solid residues for further liquefactions.

Key-words: liquefaction, biomass, bio-oil, operating conditions

Index

Table of Figures

Table Index

List of acronyms and symbols

CO_2 – carbon dioxide

$GtCO_2e$ – carbon dioxide emissions in gigatons

OECD – Organisation for Economic Cooperation and Development

BRIICS – Brazil, Russia, India, Indonesia, China and South Africa

ROW – Rest of the World

H_2 – hydrogen

H:C – Hydrogen:carbon ratio

O:C – Oxygen and carbon ratio~

wt% - weight percentage

SCW – secondary cell walls

Sx – secondary cell wall x

HHV – high heating value

TG – thermogravimetric

OH – hydroxyl group

CO – carbon mnonoxide

H_2O – water

PTSA – *para*-toluenosulfonic acid

NaOH – Sodium hydroxide

NaCl – Sodium chloride

MLA – methyl-levulinate

2-EH – 2-ethylhexanol

μ - dynamic viscosity

SD – standard deviation

ρ – density

ν – kinematic viscosity

Nx – Reaction Nx

T – Temperature

t – time

ppm – parts per million

m – mass

1. Introduction

Fossil fuels, like natural gas, coal and oil are the base of all modern societies by being the main sources to produce the energy required to fuel all types of industries. They are mostly formed by carbon, hydrogen and oxygen and are the result of the deposition of organic material over a million years. While coal and gas promote the generation of power, oil tends to be used as transportation fuel. However, fossil fuels are not an infinite resource, and are responsible for the emission of greenhouse gases like carbon dioxide (CO_2), that can cause irreversible damage to our planet**[1]**. In Figure 1, the evolution of the emission of this type of gas is illustrated by region.

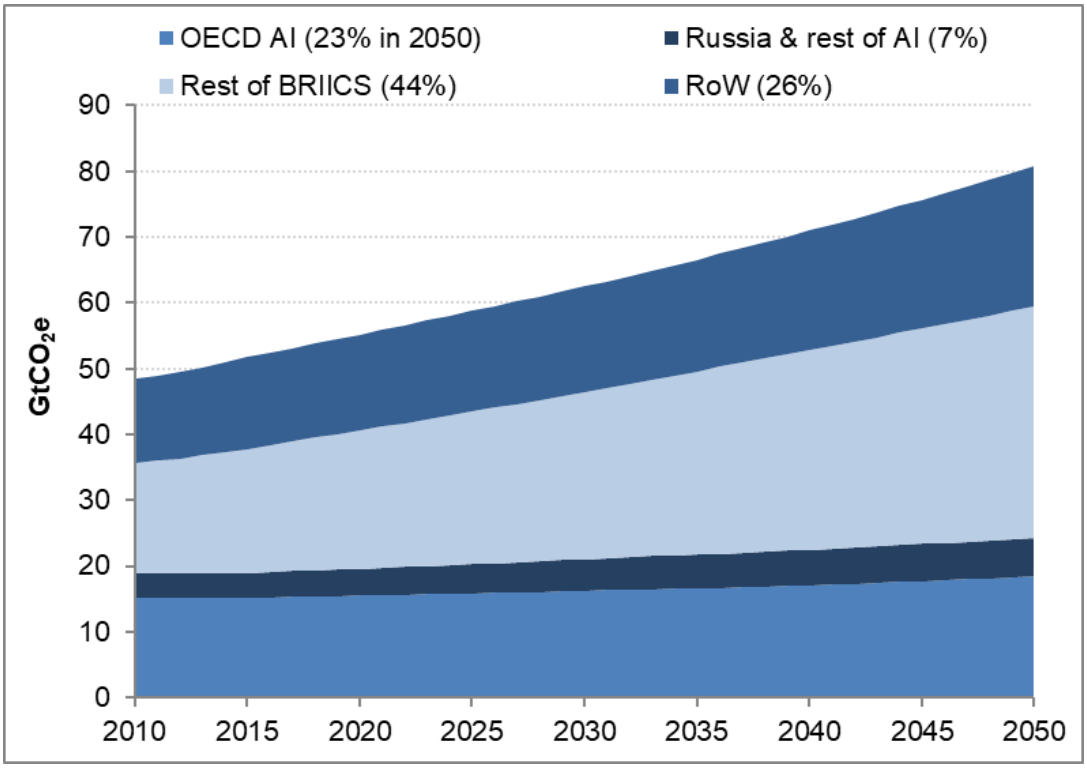

Figure 1 - Greenhouse CO_2 emissions by region in giga tonnes of CO_2 equivalent ($GtCO_2e$). OECD - Organisation for Economic Cooperation and Development; "OECD AI" stands for the group of OECD countries that are also part of Annex I (AI) of the Kyoto Protocol; BRIICS - Brazil, Russia, India, Indonesia, China and South Africa; ROW – Rest of the World [2].

The Organisation for Economic Cooperation and Development (OECD) elaborated an environmental outlook where the organisation stated that the greenhouse gas emission is expected to grow 50% until 2050 powered by a 70% growth in energy-related CO_2 emissions**[2, 3]**. The current concentration of CO_2 in the atmosphere lays in 400 ppm, 50 ppm below the limit. It is of great importance to keep this value under the limit as it provides a 50% chance of stabilizing the climate at 2 ºC global average temperature increase. Accordingly to the OECD environmental outlook, a greenhouse gas concentration of 685 ppm will be set in 2050 resulting on the possible raise of 3-6 ºC by the end of the century.

By analysing Figure 2 that presents the production of CO_2 by each reported source, it is possible to conclude that industrial processes are the bigger contributors to these type of emission**[4]**.

In 1990, chemical industry was accounted for 14% of the total greenhouse gas emission to the atmosphere. Following this alarming numbers, efforts are being made to study and develop cleaner and safer technologies, waste-recycling processes and new products to protect the environment and to increase the efficiency of energy processes. To restrain dependency on fossil oil-derived products, innovative conversion techniques are being developed with the purpose of converting lignocellulosic biomass into useful and added-value products such as biofuels. This type of fuels tend to have a relatively high OH value, a low acid number and a functionality value between 2 and 3 meaning the presence of 2 to 3 functional groups in a molecule**[5]**.

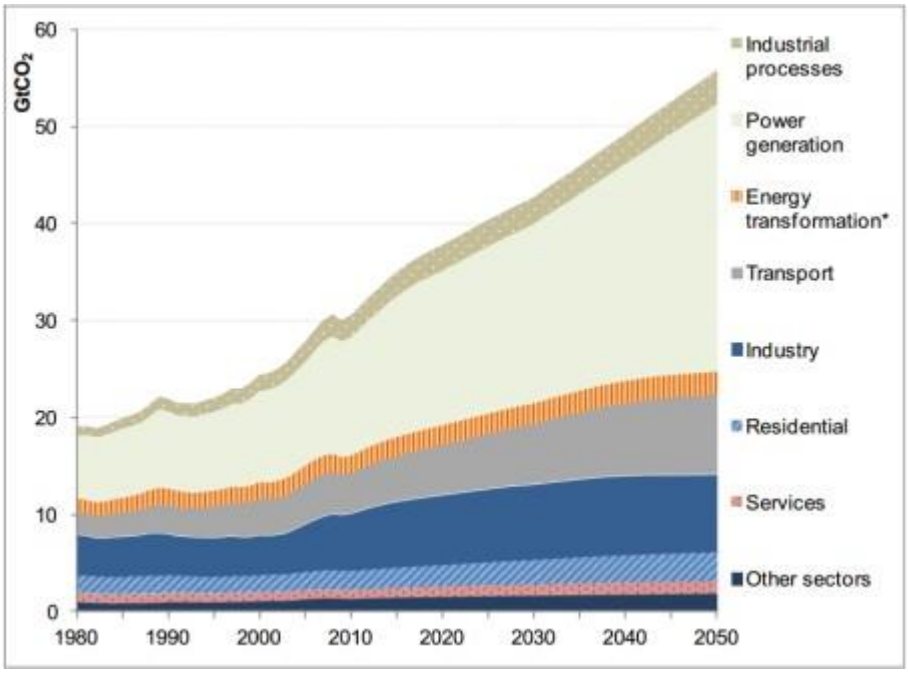

Figure 2- Global CO2 emissions by source (Baseline, 1980-2050) where the category "energy transformation" includes emissions from oil refineries, coal and gas liquefaction [2]

In the following chapters, lignocellulosic biomass background history will be checked followed by a discussion,that will aboard subjects like where it can be found and how it can be used to produce biofuel.

1.1. The Forest as a renewable chemical source

In 2018 about two thirds Forests of Portugal land area was covered by forests and wooded land. In Figure 3 the surface ratio of land use is presented by occupation classes **[6]**.

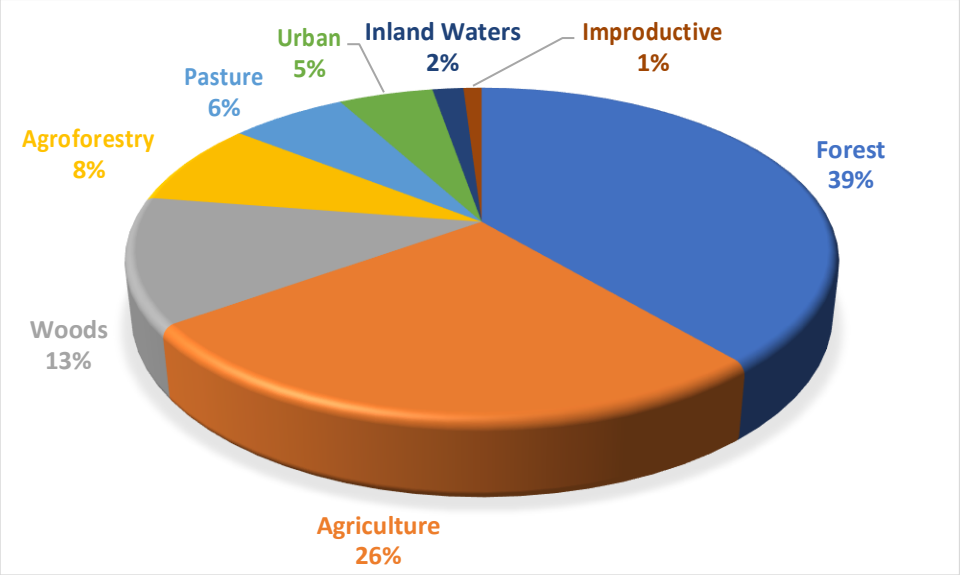

Figure 3 - Portugal land distribution in 2018 ***Fonte****: INE, I.P./DGT, Estatísticas de Uso e Ocupação do Solo 2018.* ***[6]***

Solar, wind and hydroelectric renewable energetic sources are the bigger alternatives to fossil fuel while biomass stands as the major hydrocarbon source alternative to crude oil. Biomass corresponds to all the biological material derived from recently living organisms that can be used to produce sustainable chemicals and fuels. The first response to the non-sustainability of oil supplies and the rise of CO_2 emissions was relied on a bio-based economy running on vegetal oils and sugars derived from starch or sucrose but this solution entered in the direct competition with the food chain contributing, directly or indirectly, to one of the world's biggest dilemna, food vs fuel. Facing this obstacle, the scientific community turned their focus to an underappreciated abundant biomass source: plants**[7]**.

Plant biomass is found in the wood and in the bark of the trees. Nearly 70% of plant biomass is composed of plant cells which contain the lignocellulosic matter needed to produce biological versions of common chemicals and polymers. It is estimated to be globally generated around 10 to 200 gigatons of biomass which surpasses the annual production of oil barrels that stands at 4 gigatons. Even though not all this generated biomass can be used, even a small fraction of it can be presented as a viable alternative source to fossil oil.

1.1.1. Biomass Sources

The sources of plant biomass to produce added-value chemicals are the same sources used for energy production with them being the residues of forest and agricultural industries (Figure 4), dedicated crops and residues from forest cleaning processes. Forest industry is defined by all the industry sectors that use and transform all kind of wood into increased value materials. As seen in Figure 3, Portugal possesses a fine percentage of land area occupied by forest and wood pastures allowing the country to be a potential producer of biomass derived chemicals.

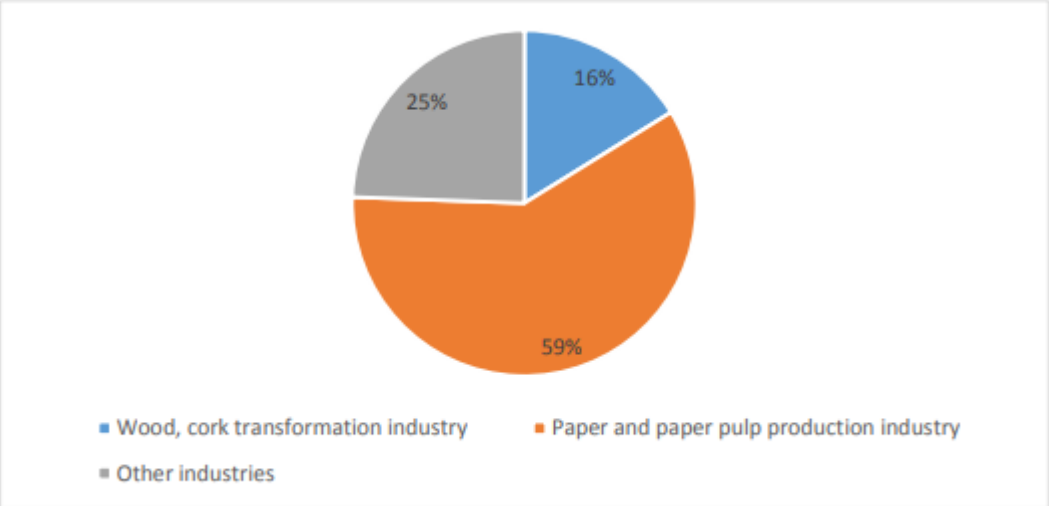

Figure 4 - Main producers of non-hazardous wood residues in Portugal in 2013 - Source: Instituto Nacional de Estatística

Regarding the biomass source, different generation biofuels can be made**[8]**. First-generation fuels derive from edible feedstock and forest trees but directly compete with the food industry, while second-generation fuels origin from non-edible parts of crops, forest residues and energy crops give no competition to the food industry. The third-generation fuels derive from macro and micro algae that use CO_2 from the atmosphere or from industrial emissions for growth. They do not compete with agricultural land and are expected to hit higher yields per hectare while yielding carbohydrates, proteins, vegetable oils, biodiesel, and hydrogen (H_2) gas. At last, the fourth-generation biofuels derive from previously modified organisms to obtain better yields but is yet to be used in large scale.

1.2. Biomass

Biomass has one perk that immediately stands out which is it being carbon neutral**[9]**, which means it does not add net CO_2 to the atmosphere when burned and its estimated that almost half of the organic carbon in the biosphere is present in the form of cellulose**[10]**. Another advantage is its low H:C and high O:C ratios that makes it suitable for producing fuels**[8]**.

Lignocellulosic biomass is known to be 35-50wt% cellulose, 20-35wt% hemicellulose and 10-25wt% lignin**[10].** It can also be found traces of suberin and nitrogen with the latter being the vital nutrient for biomass as it contributes to the energy value by not oxidizing when combusting the biomass**[11]**. The amount of carbon can be estimated from the ratios of the three main components of lignocellulosic biomass. In herbaceous plants, the carbon amount is low with the lignin content being high**[11]**.

Plant cell walls present a multi-layered structure with a middle lamella and a primary cell wall being overlaid by three layers of secondary cell walls (SCW) – S1, S2 and S3 – with S2 as the thickest. The layer above referred as "middle lamella" is not a real layer in the physical sense but a mix of filling materials like tannin. It was also mentioned previously that S2 is the thickest secondary cell wall, and it is also where the lignocellulosic content can be found – cellulose, hemicellulose and lignin – which accounts for more than 15% of the dry weight of the cell wall. Here, cellulose functions as a basic skeleton, hemicellulose as an adhesive which will combine cellulose to lignin who works as a filler**[12]**.

Biomass properties can be classified as physical, chemical and thermal. The last one mentioned is the one of most importance since it carries the property that defines the ability to operate as a fuel – high heating value (HHV). It measures the amount of energy that is released during combustion until all carbon is converted into dioxide carbon and all hydrogen into water**[13]**.

1.2.1. Cellulose

Cellulose is the most abundant organic compound in biomass as it carries 35-50% of the dry wood weight. It's a high crystalline polymer of D-anhydroglucopyranose $(C_6H_{10}O_5)_n$ units linked together by long chains of (1,4)-glycosidic bonds. Its tight hydrogen bonding network and van der Waals intramolecular forces provide stabilization to cellulose allowing it to function as the biomass skeleton and notoriously resistant to hydrolysis**[14]**. These anhydroglucose units are formed when the glucose molecules lose one molecule of water. Cellulose stands as a high weight amphiphilic molecule with a high degree of polymerization. It also becomes more soluble with the increase of temperature**[11]**.

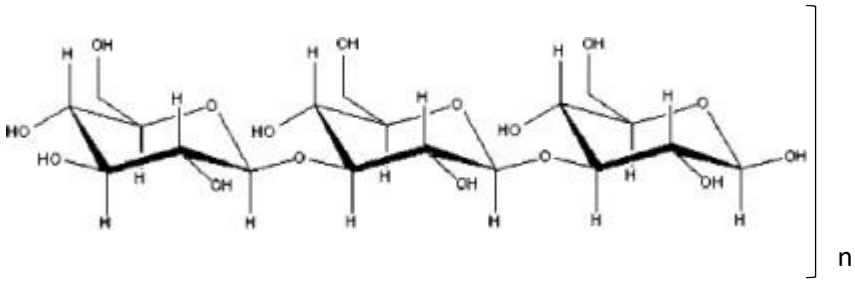

*Figure 5 - Molecular structure of cellulose **[15]***

1.2.2. Hemicellulose

Hemicellulose is the second most abundant organic material in biomass and is an amorphous polysaccharide but composed by xyloglucans, xylans, "mannans", "glucomannans" and β-(1,3 and 1,4)-glucans**[16]**. It can be found in the primary and the secondary cell wall with his main function being strengthening the cell walls by interacting with cellulose and lignin as illustrated below in Figure 6.

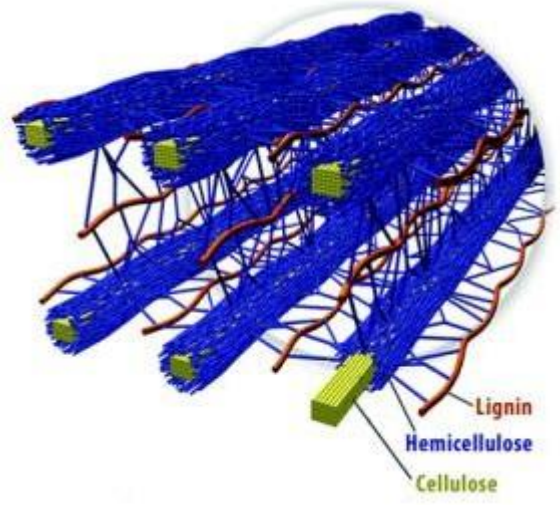

*Figure 6 - Biomass spacial arrangement **[17]***

1.2.3. Lignin

Lignin is a complex macromolecule with high chemical functionality, and it can be found mainly in the middle lamella and primary wall of xylem or suberous tissues **[18]**. Lignin can be classified following its plant family: softwood (gymnosperm), hardwood (angiosperm) and grass (graminaceous). Lignin's chemical composition varies with each family plant.

Lignin is composed of phenylpropane units (C3-C6) of p-coumarilic, synapilic and coniferilic alcohol (Figure 7). Coniferyl is the main component of softwood lignin and one of the building blocks of hardwood lignin alongside synapil alcohol.

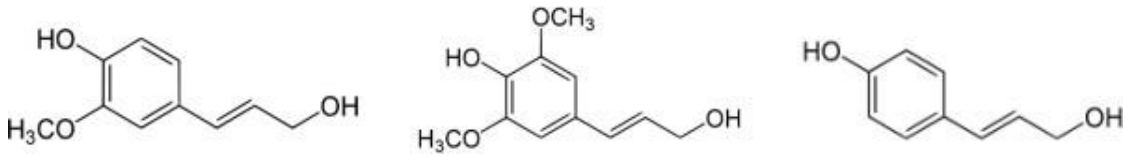

Figure 7 - Conyferil, sinapyl and coumaryl alcohol, respectively

When thermally decomposed at high temperatures, lignin forms free phenol radicals through repolymerization and condensation leading to a solid residue **[19]**.

1.3. Lignocellulosic Biomass Liquefaction

Solvent liquefaction of lignocellulosic biomass is a promising route to produce biofuels and bio-based materials under moderate reaction conditions (Figure 8) and it consists in the liquefaction with an organic solvent and acid catalyst**[16]** at elevated temperatures. Thermochemical liquefaction gained attention in the past to produce artificial coal and then, through the addition of carbon monoxide and hydrogen, to convert biomass into biofuels**[20]**. Apart from the studied type of liquefaction, different liquefaction techniques are performed for certain target products such as hydrothermal liquefaction, co-solvent liquefaction, microwave-assisted liquefaction and plasma electrolytic liquefaction which are briefly reported on Table 1.

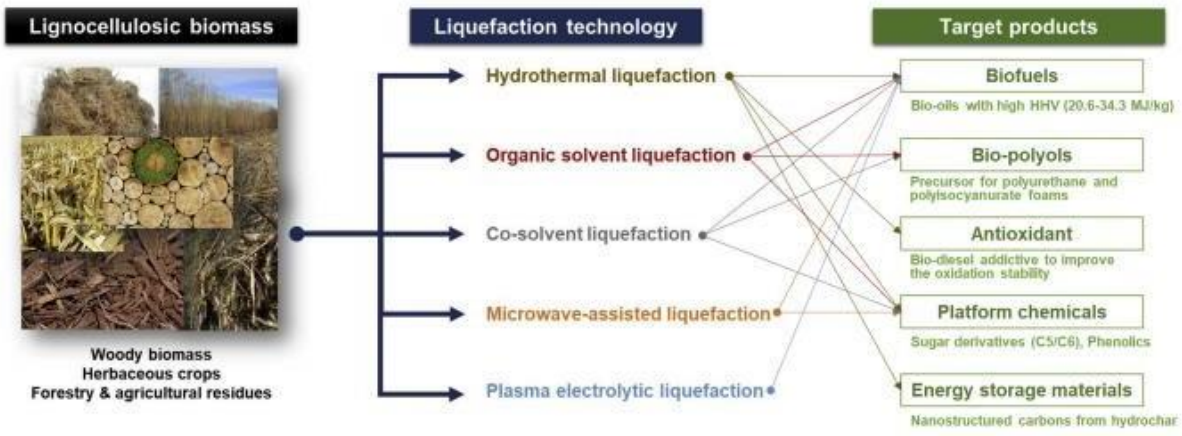

Figure 8 - Different liquefaction techniques target products [7]

Table 1 - Characteristics of different liquefaction techniques

	Description	Solvent	Main Products	Advantages
Hydrothermal Liquefaction	Liquefaction with water as solvent	Water	Bio-oil; Water soluble products; hydrochar; gas	Unnecessity to dry the biomass
Co-solvent Liquefaction	Liquefaction in organic solvent-water mixture	Water/Ethanol; Water/Methanol	Bio-oil; char; gas	Cheap; Eco-friendly; Solvent low critical point
Microwave assisted liquefaction	Liquefaction with microwave heating	Glycerol; Methanol; Ethanol; Water	Bio-oil; Water soluble products; solid residue; Gas	Heat provided to full biomass volume; Unnecessity to dry the biomass
Plasma electrolytic liquefaction	Liquefaction on electrolytic plasma	Polyethylene glycol; Glycerol	Bio-oil; Solid residue; Gas	High efficiency; eco-firendlier process

Targeting the decomposition of cellulose yields polyols, alcohols and carboxylic acids while targeting lignin's decompositions will lead to a phenolic compound**[10]**. Biomass liquefaction targets biofuels (bio-oils with high HHV), bio-polyols, antioxidants (bio-diesel), platform chemicals (sugar derivatives) and energy storage materials (nanostructured carbons).

The direct liquefaction of lignocellulosic biomass requires the use of strong liquid acids (ex: sulphuric acid) or bases (ex: sodium hydroxide) as catalyst as cellulose's crystalline structure provides resistance to hydrolysis in water**[10]**. The liquefaction process with acid catalysts undergoes at atmospheric pressure and stands as the breakage of the lignocellulosic material into smaller molecules is favored by the solvent**[21]**. When liquifying wood, in the presence of organic solvents, solvolysis occurs**[22]**. The solvent's main functions in this process are to solubilize the products while dispersing the reaction intermediates with high molecular weight and preventing the formation of coke while stabilizing the intermediates through hydrogen donation**[23]**. The more suitable solvents are alcohols such as glycerol and 2-ethyl-hexanol. Studies suggest that the liquefaction of biomass with an acid catalyst and organic solvent splits into two stages, a first and faster stage where the lignocellulosic content is removed from the amorphous regions and a second and slower stage where cellulose's stable crystalline regions are degraded**[24]**. This different stages exist due to the chemical composition of the lignocellulosic content. Hemicellulose and lignin present a more amorphous form making them easier to liquefy while cellulose has a more stable crystalline form making it harder to break and react. With this information, its possible to understand that the feedstock type greatly affects the course of the liquefaction reaction.

The reaction product called bio-oil, is a liquid mixture of oxygenated components containing one carboxyl group, one carbonyl group and one phenolic group - all deriving from biomass depolymerization and fragmentation**[21]**. The water extraction of this bio-oils leads to an organic and an aqueous extract. The first one reveals high phenolic concentration and low antioxidant activity while the latter shows the opposite, low phenolic concentration but high antioxidant activity**[21]**. The water extraction of liquefied products allows to separate the more

polar compounds with reports of this leading to products with superior HHV once compared to the raw and the already liquefied biomass**[13]**. This is believed to be due to a larger amount of carbon and hydrogen on the product after the removal of most of the oxidized compounds and formation of new C—C bonds. Its expected for the liquefaction product to have an oxygen content ranging between 12 and 20%, H:C ratio ranging between 1 and 1.3 and an average molecular weight of around 300**[13]**. Its HHV value should also be superior to 40 MJ Kg^{-1}. As mentioned previously, bio-oils possess a considerable amount of phenolic content which can be used as phenol substitutes for producing resins and its antioxidant property allows it to be used to produce phenolformaldehyde. The bio-oil low oxidation stability can be developed to become a bio-diesel additive**[16]**.

Prior to this findings, in 2009, Zou et al. studied, by thermogravimetric (TG) analysis, the effect of three alcoholic solvents: monohydric n-octanol, dihydric ethylene glycol and trihydric glycerol**[25]**. This study showed that there were three stages during biomass liquefaction: biomass dehydration, valorisation of alcoholic solvents and biomass alcoholysis. Although alcoholic solvents have shown obvious reactive activity, it is still not clear how they directly affect the liquefaction process. This study allowed the authors to develop a suggestion of the reactional pathway of both the cellulose and the lignin alcoholysis with an acid catalyst which are presented in figures 9 to 11.

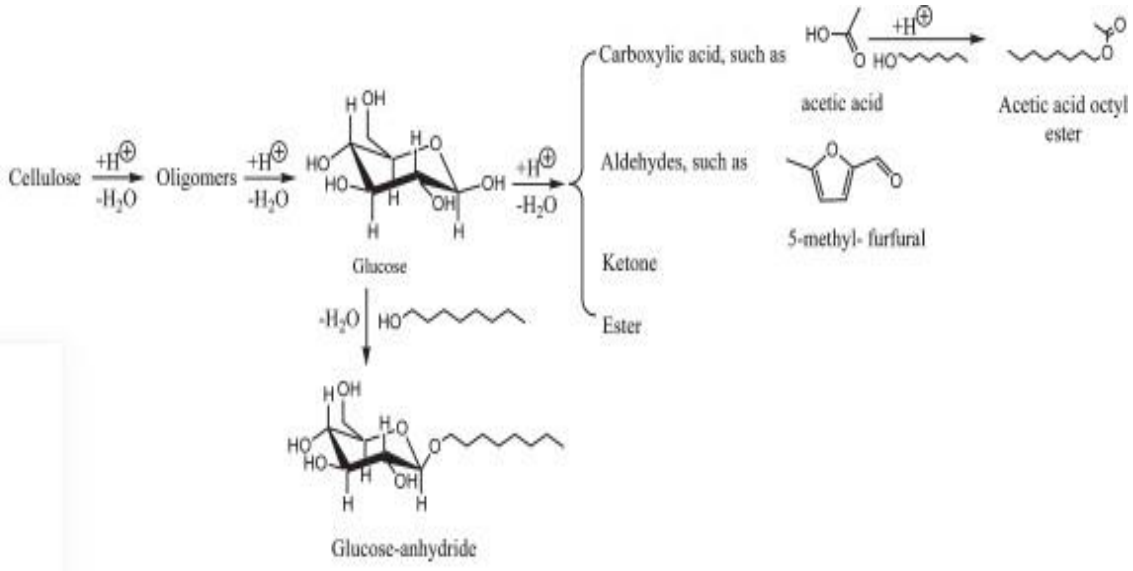

*Figure 9 - Pathway of cellulose alcoholysis by acid **[25]***

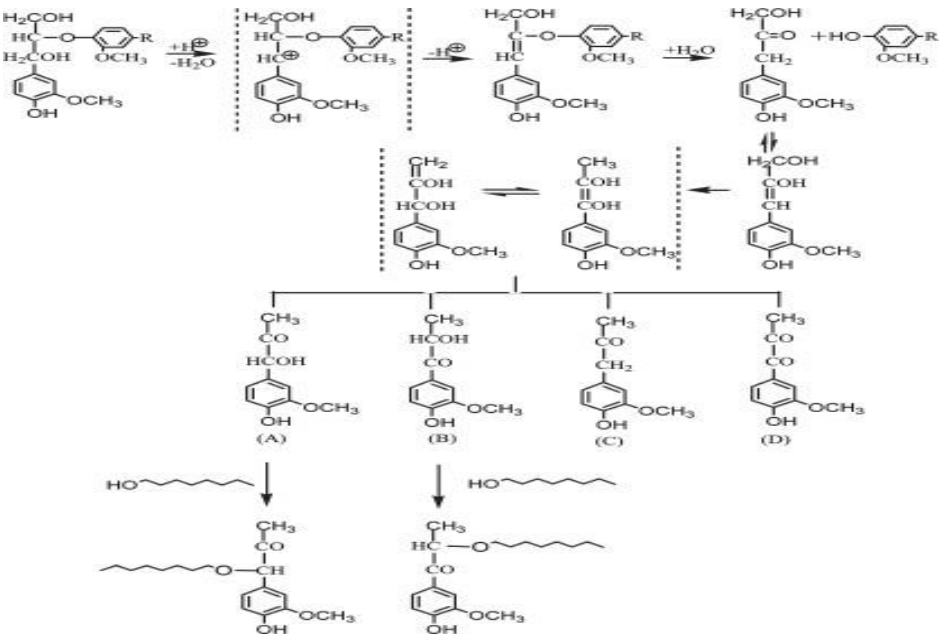

Figure 10 - Pathway of lignin alcoholysis by acid ***[25]***

In Figure 8 and 9, its possible to observe how the lignocellulosic content can work with an organic solvent with acid as a catalyst. The intermediates from the cellulose and hemicellulose degradation include glucose and xylose which are denoted as C—OH and the lignin degradation fragments are showed as L-OH. In Figure 11 its illustrated how these intermediates could combine with the solvent during the biomass liquefaction.

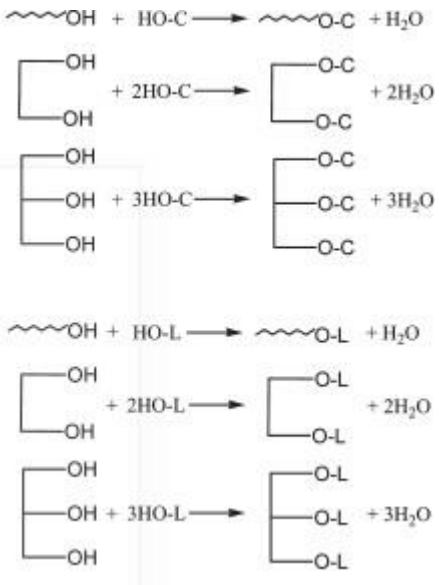

Figure 11 - Mechanism of alcoholic solvents combination with biomass liquefaction fragments ***[25]***

The solvent liquefaction of lignocellulosic biomass is affected by several factors namely the reaction temperature, the reaction time, the feedstock type, the liquor ratio, the catalyst, and the solvent used.

1.3.1. Reaction Temperature

In acid-catalyzed liquefactions, the reaction temperature is 120-180 ºC while in based-catalyzed liquefactions the temperatures rise to around 250 ºC with both undergoing at atmospheric pressure. The decomposition of hemicellulose and lignin starts at around 120 ºC leading to the formation of five-carbon sugars and some phenolic content. The liquefaction of the plant cell wall goes from the surface of the cell wall towards the centre of the S2 layer**[26]**. This five-carbon sugars are the first-step products from the direct cleavage from holocellulose by solvent degradation and have a higher thermal stability once compared to six-carbon sugars. Five-carbon sugar derivatives are abundant when working under 160 ºC, and a remarkable increase in cellulose conversion is observed at 200 ºC. Increasing the reaction temperature reduces the intermolecular forces increasing the amorphous regions of cellulose **[27]** but increasing it further than 200 ºC will lead to secondary reactions like carbonization of the liquefaction products leaving a lower bio-oil yield **[10]**. Also, a faster heating rate can reduce the recombination of initial products**[20]**.

1.3.2. Catalyst Concentration

The effect of different catalyst concentrations is also approached on this work with the literature stating that the conversion yield tends to increase with the increase of this concentration**[10]**.

In 2016, Xu et al. investigated the cellulose behaviour in a methanol liquefaction in the presence of an acid catalyst**[28]**. His investigation resulted in a belief that the acid catalyst provides protons for the glycosidic bonds cleavage. These bonds can be broken by nucleophilic attack from methanol's hydroxyl (OH) functional group producing a leaving group and a neutral hydroxyl group by C-O bond degradation. This results in cellulose releasing C6 sugar derivatives.

1.3.3. Reaction Time

The reaction time is an important variable in the liquefaction of biomass. It would be to expect that increasing the reaction time would increase the bio-oil yield, but it would favour secondary reactions like repolymerization leading to a lower yield**[21]**. This yield lowering is due the formation of humins**[29]**.

Shorter reaction times should be applied with much higher reaction temperatures to prevent side reactions like repolymerization.

1.3.4. Feedstock type

As priorly mentioned, hemicellulose and lignin present a more amorphous form making them easier to liquefy while cellulose has a more stable crystalline form making it harder. Their different reactivities create a wide list of possible reaction products. For instance, the decomposition of cellulose tends to yield polyols, alcohols, and carboxylic acids while the decomposition of lignin yields primarily phenolic content**[10]**.

The chemical differences between the lignocellulosic content leaves them to be liquified at different stages of the reaction. This content varies with almost every feedstock type available from cork to eucalyptus. The distribution of cellulose, hemicellulose and lignin will determine the distribution of the obtained products and time of reaction need. Theoretically, a biomass source with a less stable crystalline cellulose region will liquefy faster than a more stable one**[30]**. Zheng et al. studied the liquefaction of bagasse and wheat straw. The liquefaction of the latter produced the lowest yield due to its lower amorphous area and higher crystalline area.

1.3.5. Liquor Ratio

The reaction liquor ratio consists in the solvent:biomass ratio. A ratio lower than 3:1 results in higher viscosity products**[31]** while increasing this ratio leads to a higher yield and a higher percentage of acid-insoluble lignin**[22]**. The importance of this ratio was studied by Yang et al. who treated wheat straw with polyethylene glycol on a ratio below 3 resulting in a yield decrease due to the solvent incapability to access the biomass. Yang and coworkers also found that high amounts of biomass lead to a drastic increase in viscosity.

1.3.6. Solvent Selection

The liquefaction of lignocellulosic biomass undergoes solvolysis when working with organic solvents, as mentioned above, with organic alcohols being the most suitable solvent.

Simpler alcohols like methanol, ethanol, propanol and butanol provide higher liquefaction yields, while alcohols with longer chains and organic acids acids lead to a higher amount of residue. Despite this advantage, its lower boiling points could result in their evaporation before the beginning of the liquefaction process**[32]**.

Despite it already had been found a suitable solvent for biomass liquefaction, the scientific community kept pushing efforts to try and develop another route when deciding the solvent.

Some of these alternatives will further be briefly reviewed on this work namely the use of sub-/supercritical alcohols and the use of an ionic liquid. Another alternative is the hot compressed water which has been proven an effective solvent for biomass liquefaction due to its low dielectric constant, fewer and weaker hydrogen bonds, higher isothermal compressibility, and enhanced solubility when working with organic compounds **[33]**.

1.3.6.1. Ionic Liquids as Solvent

Ionic liquids possess some attributes that instantly make them a contender for solvent selection with them being their high acidic density, low corrosivity and uniform active centers**[24]**. When dissolved in ionic liquids, cellulose and cellobiose have a similar behaviour meaning the polymeric supramolecular structure fully disassemble breaking all physical protections against hydrolytic processes**[34]**. This physical barrier is overcome through the formation of a solution where the dissociated anions and electron-rich aromatic π systems can also weaken the glycosidic bonds to allow hydrolysis to occur.

Cellulose's O-sites can be classified into two groups following their basicity with the acetal O-sites the less alkaline and the hydroxyl O-sites the most. Due to the weak basicity of the glycosidic O-site, strong acids are required to activate cellulose towards hydrolysis.

This alternative route produces the same or higher yields of glucose and TRS when comparing to the conventional liquefaction. With longer reaction times, glucose formation is favoured while with shorter reaction times the production of TRS is favoured.

A great advantage of this method its his ability to recycle the ionic liquid by stopping the reaction at the cello oligomer stage and adding water.

1.3.6.2. Sub-/Supercritical fluid as Solvent

Subcritical fluids are substances at temperatures and pressures below their critical point while supercritical fluids are substances at temperatures and pressures above the same point. This type of fluids unique transport properties, gas-like diffusivity and liquid-like density, and ability to dissolve materials that do not normally dissolve in conventional methods sparked attention**[33]**. But this were not the only advantages as sub-/supercritical fluids are easy to separate from the bio-oil through a simple alcohol drying, show lower corrosive risk when compared to water and provide hydrogen throughout the reaction preventing any secondary reactions like repolymerization and carbonization**[16]**.

Supercritical ethanol appeared to be a promissor solvent for biomass liquefaction since this physical state boosts its solubility, hydrogen donating capacity and promotes the occurrence of deoxygenation reactions enhancing the bio-oil HHV value while also removing oxygen in the form of carbon monoxide (CO), CO_2 and water (H_2O) leading to the production of an energy-intensified bio-oil**[23]**. Its low boiling point makes it easy to recover.

1.4. Biomass Liquefaction Products

The solvent liquefaction of woody biomass allows the production of biofuels, phenolic resins **[35]** and adhesives**[24]**, polyurethane foams**[3]**, carbohydrates**[9]**, among others. Phenolic resins and adhesives can be prepared with phenol liquefaction while polyurethane foams are obtained by reacting isocyanates with alcohols products**[27]** with polyol being the precursor of the latter.

Targeting the decomposition of cellulose yields polyols, alcohols and carboxylic acids while targeting lignin's decompositions will lead to a phenolic compound**[10]**. Biomass liquefaction targets biofuels (bio-oils with high HHV), bio-polyols, antioxidants (bio-diesel), platform chemicals (sugar derivatives) and energy storage materials (nanostructured carbons)**[6]**.

It has been noted that lignin has a similar structure to phenolic resin leading to believe that lignin could substitute phenol in the synthesis of phenol formaldehyde resins through biomass liquefaction**[9]**. The production of phenol formaldehyde resins give rise to three concerns: its relatively high viscosity values, high hydrophilic character and, relatively low cross-linking density. Further condensation of the phenol liquified biomass with formaldehyde led to synthesize novolac and resol phenolic resins efficiently converting the unreacted phenol into resins. This bio-based resins have already achieved a superior biodegradability when compared to petroleum based resins**[35]**. Novolac resin is a thermoplastic resin synthesized with a phenol-to-formaldehyde molar ratio greater than one under acidic conditions while resol resin is thermoset and synthesized with phenol-to-formaldehyde molar ratio below one under alkaline conditions with an extra step of neutralizing the acidic liquefied biomass. Mishra and Sinha **[24]** reported the preparation of a polyurethane wood adhesive from waste paper and castor oil by pre-treating the raw materials and undergoing the reaction for 2.5 hours at 150 ºC with ethylene glycol as solvent and 0.5wt% of p-toluenesulfonic acid (PTSA) as catalyst. After the removal of the unreacted solvent, a 93% glycoside yield was obtained. The glycoside was then used to synthesize polyols with castor oil reacting them for 1 hour at a temperature range between 220 and 250 ºC with lithium hydroxide as the catalyst. Polyols with higher hydroxyl values showed lower viscosity levels and higher adhesive joints lap shear strength. The obtained polyol was finally mixed with Toluene diisocyanate (TDI) obtaining the desired polyurethane wood adhesive which showed good water resistance and moderate resistance to acid treatment.

Another type of resin can be obtained from liquefied wood. Epoxy resins are a thermosetting polymer which results from reacting epoxide with a curing agent like polyamine being the most widely used resin made through condensation of epichlorohydrin with bisphenol A or diphenol propane**[9]**. This new type of resin has many possible applications going from surface coating materials to engineering adhesives. In 2010, Wu and Lee looked to evaluate epoxy resins from liquefied bamboo**[29]**. They started their experiment by reacting epichlorohydrin with bisphenol A, 5:1, at 110 ºC for 2 hours while stirring and adding drops of aqueous sodium hydroxide (NaOH). This was followed by the addition of the liquefied bamboo and some extra epichlorohydrin. The epoxy resin was then obtained after filtration of the by-product sodium chloride (NaCl) and removal of unreacted epichlorohydrin and water through reduced pressure

distillation. The resulting resin finally revealed similar curing behaviour comparing to the commercial petroleum-based epoxy resin and a lower thermal degradation as well.

Biomass liquefaction products can also be used as an antioxidant material due to its oxidative stability that could work as a bio-diesel additive**[9]**. Another popular product is methyl-levulinate (MLA) which derive from carbon hydrates. MLA is composed by small but thick ester chains allowing it to be used as fuel additive **[9]**.

On some reactions, "hydrochar" is produced and it can be used as a supercapacitor resource through chemical activation with KOH, H_3PO_4 and CO_2**[9]**.

Lignocellulosic's biomass dominant presence of oxygen-rich cellulosic carbohydrates leads to oxygenated molecules with carboxyl, keto and/or hydroxy groups after being subjected to depolymerization and degradation processes. Although, in order to yield targeted value-added chemicals, a deoxygenation is required which will be accompanied by the formation of new C-C bonds. Another performance-increase was associated to adding metal ions to the catalyst support. This will allow to modulate the pH on the catalyst surface facilitating the biomass degradation while also reducing the carbon deposition by both the active and supportive metal sites**[9]**.

2. Experimental Procedure

As it was mentioned in the introduction, lignocellulosic biomass acid liquefaction undergoes under ambient pressure with temperatures ranging from 120 to 170 ºC. On this work, the catalyst used was PTSA and the solvent was the polydric alcohol 2-ethylhexanol (2-EH) with a 5:1 liquor ratio. Three catalyst amounts were tested, 0.5, 1.75 and 3wt% (in relation to the solvent plus biomass total mass), for the reaction times of 30, 105 and 180 minutes. A set of 17 reactions was prepared to better understand how different reaction media alters the course of biomass solvent liquefaction.

2.1. Biomass Preparation

The first step of this work experimental procedure layed on preparing the biomass source, in this case, cellulose.

Cellulose was left in boiling water in order to soft the tissue facilitating the cutting step. When soft, the biomass was shredded spliting the biomass into smaller size particles.

The wet biomass was then left drying at 80 ºC until it dried completely.

2.2. Biomass Liquefaction

For each experiment the following procedure was addopted varying the wt% of catalyst, reaction temperature and reaction time:

1. 60g of the already dry biomass was added to a mixture of 2-ethylhexanol (300g) and p-toluenesulfonic acid and placed inside a glass reaction vessel;
2. The reaction vessel was then placed on a heating mantle, to be heated to the desired temperature;
3. The reaction vessel was kept under nitrogen atmosphere through all experiments;
4. For temperature control, a thermocouple directly connected to the heating “blanket” was used, and a stiring shaft connected to a stir engine “IKA Microstar 30 control” was employed for continuous stirring. A glass condenser was also used.
5. As soon as the temperature was reached, the counter was started.

In Figure 12, the experimental setup assembled for each experiment is presented.

Figure 12 - Liquefaction Setup from the author

The reaction temperature was controlled through the thermocouple which was attached to the heat source to control any temperature flutuations. The stir engine worked on 250 rpm throughout all experiments. The nitrogen source was restrained to about one released bubble per second.

At the end of each experiment according to the selected reaction time, the solution was left cooling *in situ* until an 80 ºC temperature was reached.

2.3. Bio-oil Filtration

After cooling, the solution followed filtration to separate the produced bio-oil from the unreacted solid residues. This was performed under vacuum using a kitasato, a Buchner funnel and paper filter. The washing was thoroughly made with acetone.

After filtration, the liquid bio-oil was weighted and labeled while the solid residue is left to dry at 80 ºC to remove traces of acetone from the wash. The solid residue was weighted after dried and with its value, the liquefaction yield was calculated through the following equation:

$$\eta = \left(1 - \frac{residue\ mass}{biomass\ initial\ mass}\right) \times 100$$

2.4. FTIR analysis

The Fourier-transform infrared (FTIR) spectrophotometric analysis was obtained using a Perkin Elmer, Spectrum Two, equipped with a UATR Two accessory at a 4 cm^{-1} resolution and 8 scans of data accumulation. These analysis were performed at Centro de Recursos Naturais e Ambiente (CERENA) of Instituto Superior Técnico.

Figure 13 - UATR Two accessory

2.5. Elementar analysis

The elementar analysis was performed by LAIST (IST's analysis laboratory).

2.6. Viscosity analysis

The viscosity values of the bio-oils were determined using a Julabo18V rheometer alongside a ViscoClock Plus from SI Analytics. On this work, viscosities values from 20 to 80 ºC were studied. These analysis were performed at Centro de Química Estrutural of Faculdade de Ciências da Universidade de Lisboa.

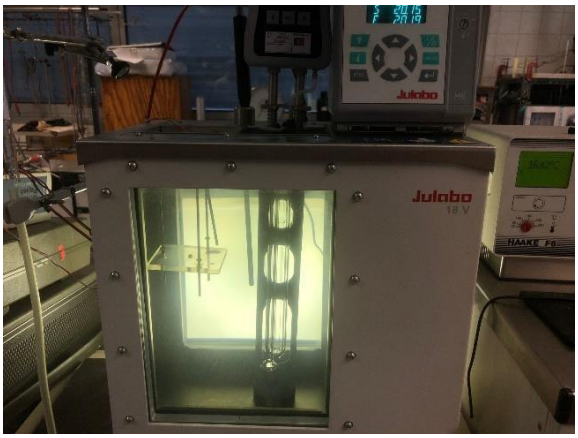

Figure 14 - Julabo18V rheometer

2.7. Density analysis

The density and speed of sound values were obtained using a DSA 5000M densimeter with a 10 to 80 ºC temperature range reported. These analysis were performed at Centro de Química Estrutural of Faculdade de Ciências da Universidade de Lisboa.

Figure 15 - DSA 500M densimeter

2.8. MODDE Software

An experimental model was created with MODDE software, version 12.1 from Sartorius Stedium Biotech. The model preparation consisted in running 17 reactions with two fixed parameters (biomass wt% and solvent wt%) and three variable parameters: reaction temperature, reaction time and catalyst wt%. The conversion yields were inserted in the model and an eighteenth reaction was performed to evaluate the model's ability to predict new data.

3. Results and Discussion

As mentioned previously, a set of 17 reactions was run varying three reaction parameters: temperature, amount of catalyst, and reaction time. All liquefactions were done with a 5:1 liquor ratio meaning 300g of solvent (2-ethylhexanol) for 60g of lignocellulosic biomass as this was the ideal massic value due the reactor volume. The obtained yields are represented below in Table 2 alongside the different reaction parameters.

Table 2 - Liquefaction set and yields

N	*T (ºC)*	*t (min)*	$m_{catalyst}$ *(g)*	$m_{biomass}$ *(g)*	$m_{residue}$ *(g)*	Yield (%)
1	120	30	1.8	60.2	57.1	5
2	120	180	1.8	60.1	53.7	10
3	170	30	1.8	60.4	47.2	22
4	170	180	1.8	60.4	47.7	21
5	120	30	10.8	60.1	44.5	26
6	120	180	10.8	60.0	39.8	34
7	170	30	10.8	60.8	21.6	64
8	170	180	10.8	60.1	9.1	85
9	145	30	6.3	60.1	41.5	24
10	145	180	6.3	60.3	30.4	50
11	120	105	6.3	61.5	39.2	36
12	170	105	6.3	60.9	21.0	65

13	145	105	1.8	60.1	47.7	31
14	145	105	10.8	60.0	28.1	53
15	145	105	6.3	60.1	25.4	58
16	145	105	6.3	60.2	27.6	54
17	145	105	6.3	59.7	25.4	58

A quick look at Table 2 allows to target *N1* and *N8* as the liquefactions with lowest and highest bio-oil yields identified in red and green, respectively.

Its expected a higher bio-oil yield with the increase of the reaction time and temperature until a certain value, from which the opposite behaviour occurs, leading to lower yields. Regarding the amount of catalyst, an increase in its concentration is believed to lead to a higher content of lignin and hemicellulose and a lower content of cellulose.

The three highest bio-oil yields resulted from reactions *N8*, *N7* and *N12* with the 170 ºC temperature being the only common reaction parameter. Although, one of the three lowest yields (*N1*, *N2* and *N4*) was also obtained at that same temperature. In fact, *N4* underwent the same reaction time as *N8* but its six times lower catalyst concentration led to a nearly four times lower bio-oil yield.

The impact of the acidic concentration can also be verified when comparing reactions *N*(1;5), (3;7), (4;8), and (13;14;15). All these combinations share the same reaction time and temperature only differing in the amount of catalyst used. Its important to recall that the three massic values used were 1.8, 6.3 and 10.8g of PTSA. Looking at Table 2, its possible to conclude that a higher bio-oil yield was obtained when using higher amounts of catalyst under the same reaction time and temperature with exception to the pair *N*(14;15). Both reaction were performed at 145 ºC for 105 minutes with *N14* having the higher amount of acidic concentration but a lower yield. This results could be explained with this reaction temperature not being favoured with an increase in the catalyst concentration.

The effect of the reaction temperature on biomass liquefaction can be evaluated when comparing the reaction pairs *N*(1;3), (2;4), (6;8), and (11;12;15). On all combinations its possible to confirm that higher temperatures often obtain higher yields. The combination *N*(1;3) underwent for 30 minutes with the lowest used catalyst concentration, and a 170 ºC temperature allowed *N3* to obtain a 21.9% yield while a 120 ºC temperature led *N1* to the lowest yield of the entire set, 5.1%. As reported earlier, lignin and hemicellulose start to decompose at around 120 ºC and only at around 160 ºC its possible to see cellulose's decomposition. With this in mind, its possible to understand how the different temperatures led to the different bio-oil yields. *N1* was not fed enough energy to start decomposing cellulose while *N3* reached a temperature where cellulose is already decomposing.

The last parameter to approach is the reaction time. The effect of this reaction variable can be observed when comparing the reaction pairs: *N*(1;2), (3;4), (5;6), (7;8), and (9;10;15). Excluding the pairs *N*(3;4) and *N*(10;15), all reactions with higher reaction time produced bio-oils with higher yield. In *N*(3;4), the reaction with lower reaction time produced the higher yield with a small difference of 0.8% while in the pair *N*(10;15) a yield difference of 8.2% was observed. *N10*, which reacted for 180 minutes, produced a bio-oil yield of 49.6% while *N15*, which reacted for almost half of the time, produced a yield of 57.8%. In the introduction of this work, it was referred that an increase in the reaction time would lead to higher yields but an excessive increase of the reaction time would lower the bio-oil yield. This can be confirmed with the results of this work by looking at the reaction trio *N*(9;10;15). All these three reactions were performed at 145 ºC with the catalyst mass being 1.75wt% only varying the reaction time: $t_{N10} > t_{N15} > t_{N9}$. The obtained values confirm that increasing the reaction time from 30 to 105 minutes led to a higher yield but increasing it to 180 minutes resulted in a lower yield but still higher than the reaction with less reaction time ($yield_{N15} > yield_{N10} > yield_{N9}$).

The bio-oils produced in reactions with a superior yield showed a darker and browner colour while the bio-oils with lower yields presented a light brown colour.

The MODDE® software allowed to validate the obtained results. With this software it was possible to evaluate four parameters: the model validity, the percent of the variation of the response predicted by the model (Q2), how well the model fits the data (R2) and the reproductibility.

A first run of the software allowed to identify reactions N10 and N14 as outliers through the spectrum of residuals vs predicted response in Figure 16.

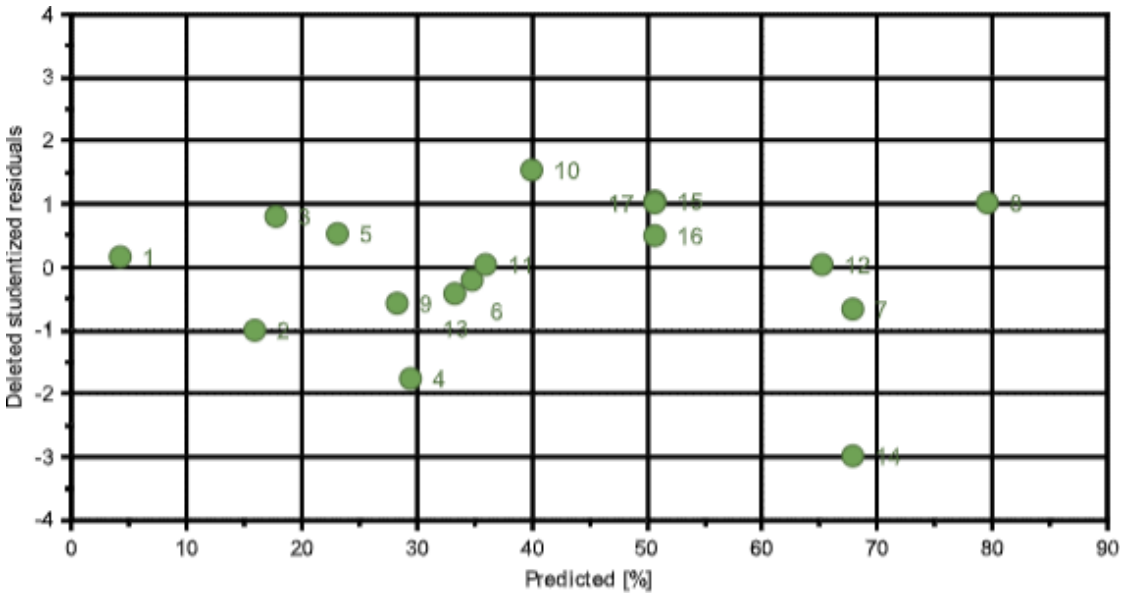

Figure 16 - Residuals vs Predicted Response (original)

With the outliers removed, the model was improved through the increase of all four parameters as it can be seen in Table 3. In Figures 17 and 18 the smaller deviation from the model can be observed without the results from N10 and N14. The obtained model validity is superior to

0.25 meaning there is no lack of fit of the model and the set's Q2 suggests the model is useful for new data prediction. Both reproductibility and R2 values obtained are high.

Table 3 - Summary of Fit

	R2	Q2	Model Validity	Reproductibility
Set with all 17 reaction	0.920	0.811	0.299	0.991
Set without N10 and N14	0.973	0.896	0.504	0.992

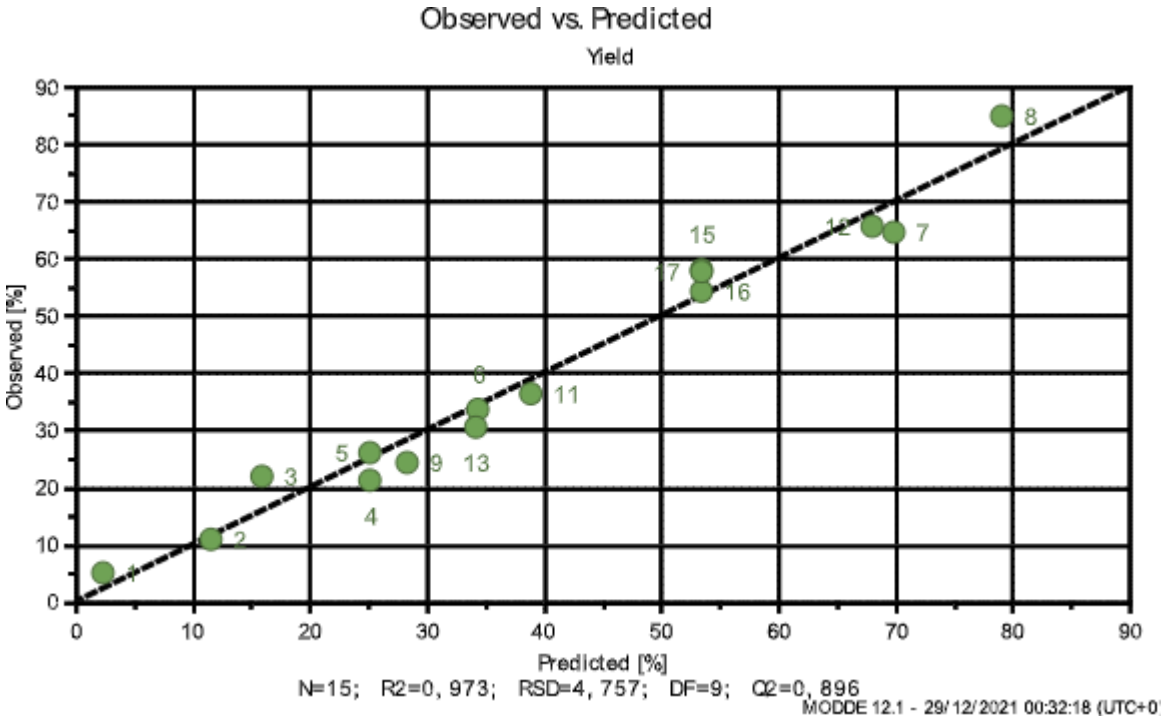

Figure 17 - Observed vs Predicted Yield (without outliers)

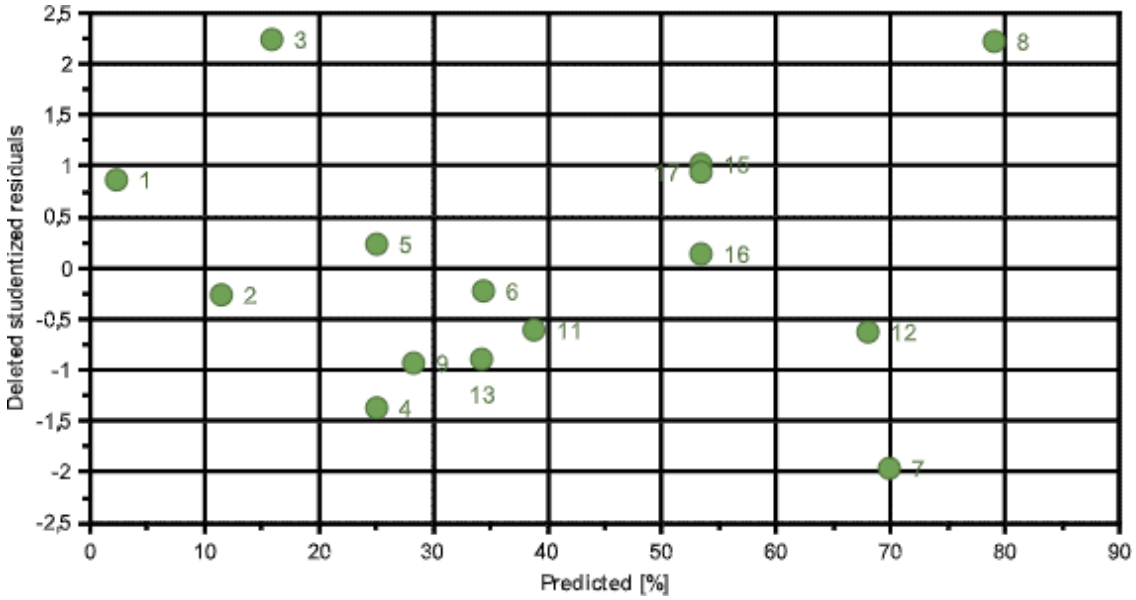

Figure 18 - Residuals vs Predicted Response (without outliers)

In order to validate the reaction set, one extra reaction was made (N18) and its yield was compared with the result obtained using MODDE®. *N18* reaction media and yield is described below in Table 4.

Table 4 - N18 reaction media and yield

N	*T (°C)*	*t (min)*	$m_{catalyst}$ *(g)*	$m_{biomass}$ *(g)*	$m_{residue}$ *(g)*	Yield (%)
18	150	140	5.4	60.3	28.3	53
MODDE® Prediction	-	-	-	-	-	46.14 – 55.34

The obtained conversion yield of N18 layed inside the interval predicted by MODDE® confirming the evaluated Q2 and model validity.

To avoid testing all products and solid residues, three reactions were chosen to study the chemical properties of the liquefied products. The three reactions are *N1* due being the reaction with lowest yield, *N8* the reaction with the highest yield, and *N18* the "control" reaction.

3.1. FTIR Analysis

All the products were analyzed with this technique and the correspondent graphs are displayed in the Appendix alongside the FTIR spectra of the used solvent and biomass. There is also the spectra of a commercial lignin sample. The spectrum of the bio-oils and solid residues from reactions *N1*, *N8* and *N18* are going to be evaluated. Below in Table 5, the relevant bands wavelenghts are illustrated.

Table 5 - FTIR Spectrum Table

Wavelenght (cm^{-1})	Group	Compound Class
3350	O-H stretch	Alcohol
1750-1650	C=O stretch	Carbonyl

Figure 19 shows that the bio-oils have a similar behaviour so Figures 20 and 21 were used to zoom in the regions of 1900-400 cm^{-1} and 3500-2500 cm^{-1}, respectively, for a better observation of the oil differences.

All graphs report less than 5 bands characterizing the bio-oils as simple organic compounds with small molecular weight. The three bio-oils share an identical "single bond area" with a strong broad band at 3350 cm^{-1} believed to be the O-H stretch of alcohol groups. Unlike *N1*, *N8* and *N18* have bands in the "double bond region". The bands in this 1750-1650 cm^{-1} region are characteristic of a carbonyl C=O stretch. In the "figerprint region" (1500-600 cm^{-1}), all bio-oils possess mutual bands in the 900-650 cm^{-1} region, which are characteristic of carboxylic acids while the peak in around 1030 cm^{-1} describes a C-O stretch in O-CH_3. Atlast, two peaks reported between 1450-1350 cm^{-1} are also common to the three oils. This peaks also suggest a C-O stretch in O-CH_3.

With the bands analysed, its possible to confirm the stretching vibrations of hydroxyl groups (3500-3200 cm^{-1}) on all three oils. *N8* and *N18* share a stretching vibration of carbonyl groups (1750-1650 cm^{-1}) that *N1* does not. The registered hydroxyl group at 3350 cm^{-1} originated from the solvent (2-ethyl-hexanol) with this band also being reported in the solvent FTIR spectra displayed in the Appendix. The carbonyl group should have been formed from the biomass degradation.

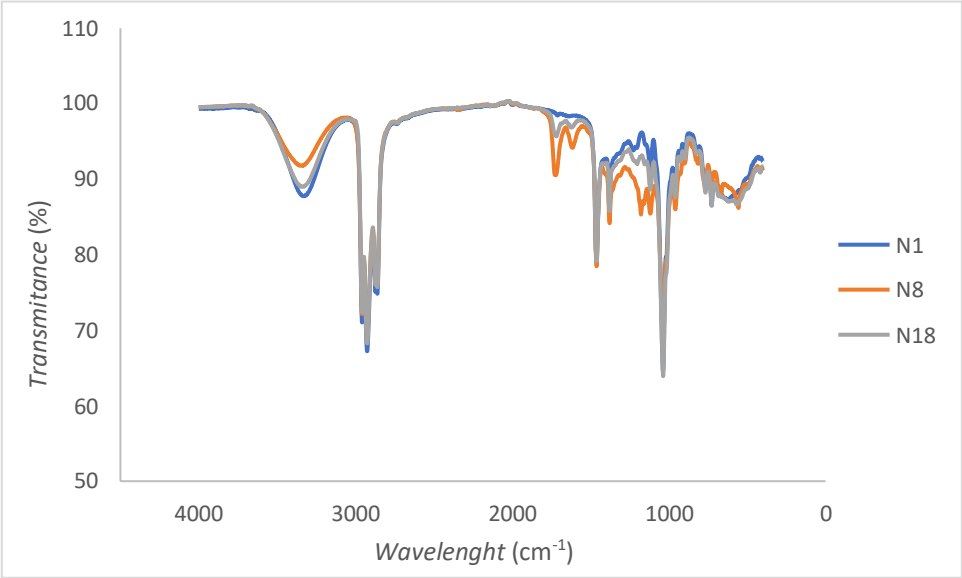

Figure 19 - FTIR spectra of N1,N8 and N18 bio-oils

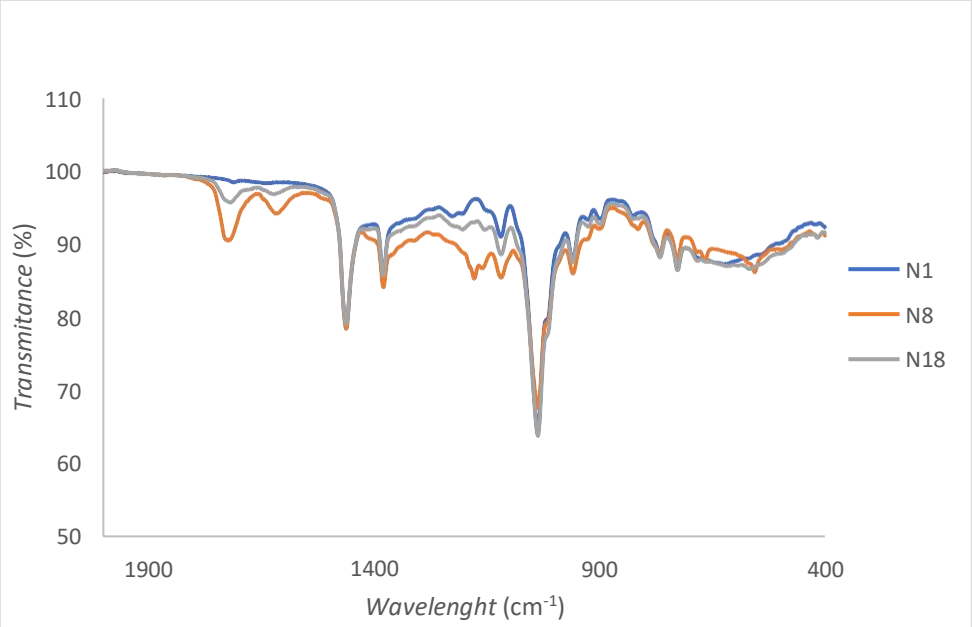

Figure 20 - FTIR spectra of N1, N8 and N18 bio-oils zoomed-in (1900-400 cm^{-1})

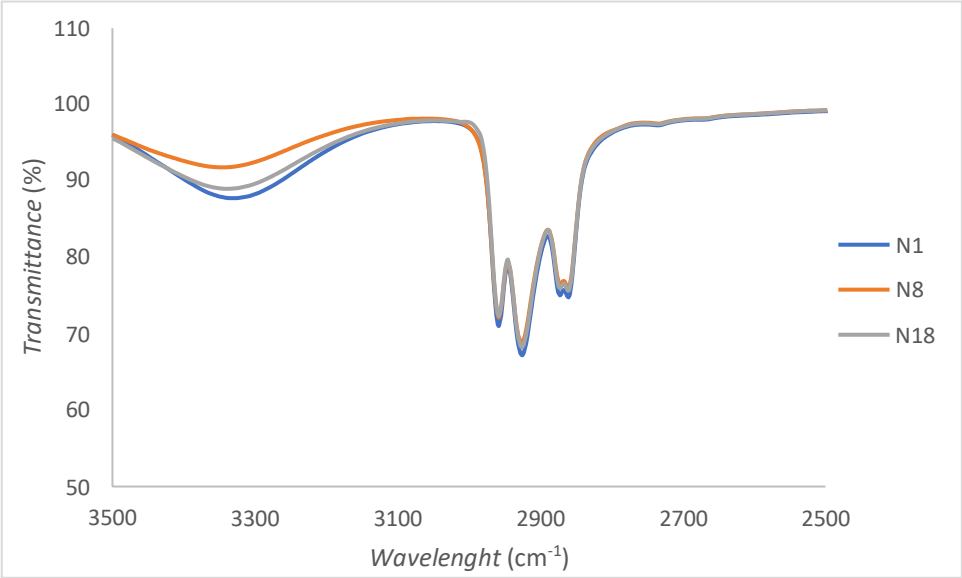

Figure 21 - FTIR spectra of N1, N8 and N18 bio-oils zoomed-in (3500-2500 cm^{-1})

Now the solid residue of the same reactions are observed below. In Figure 22, the entire wavelenght is observed and Figure 23 corresponds to the zoom in of the 1800-300 cm^{-1} region.

Like the bio-oil analysis, less than 5 bands are visualized meaning it's a simple organic compound with small molecular weight. All three residues present a broad band at around 3350 cm^{-1} which describes a O-H stretch, usually seen in alcohol groups. This stretch is likely to have origin in unreacted solvent. A C=O stretching vibration is described at 1660 cm^{-1}, a C-O stretch at 1056 cm^{-1}, and another C-O stretch characteristic in O-CH_3 at 1032 cm^{-1}. Finally, at 560 cm^{-1}, C-H out-of-plate bending vibrations are reported. This is a trait seen in organic materials.

With the bands evaluated and the graphics observed, its possible to conclude that the three solid residues share an identical band behaviour only with different intensities. Stretching vibrations of carbonyl, ether and hydroxyl groups were observed. The hydroxyl stretch vibration, as in the bio-oils, derives from 2-ethyl-hexanol. The ether group is believed to be resultant from the interaction between biomass fragments and the solvent.

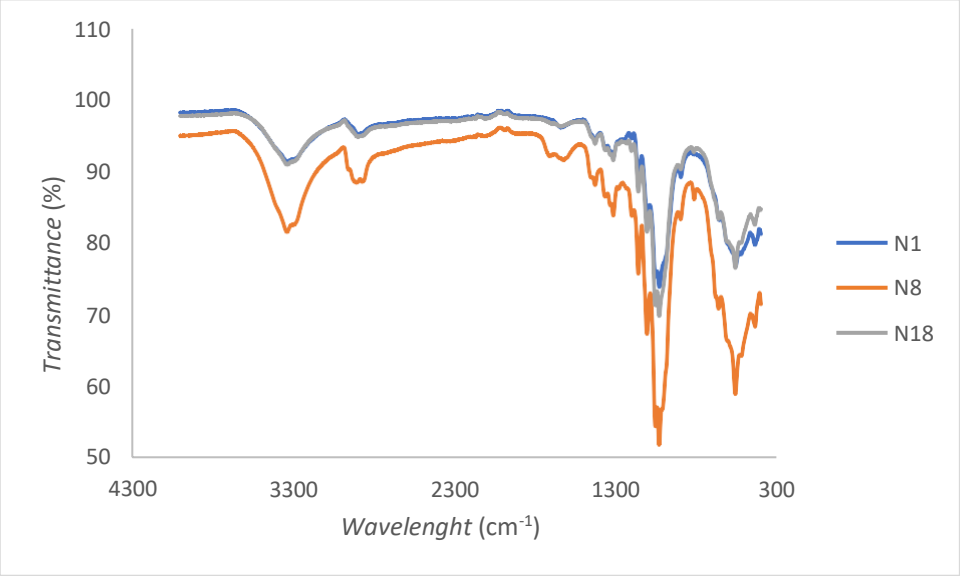

Figure 22 - FTIR spectra of N1, N8 and N18 solid residues

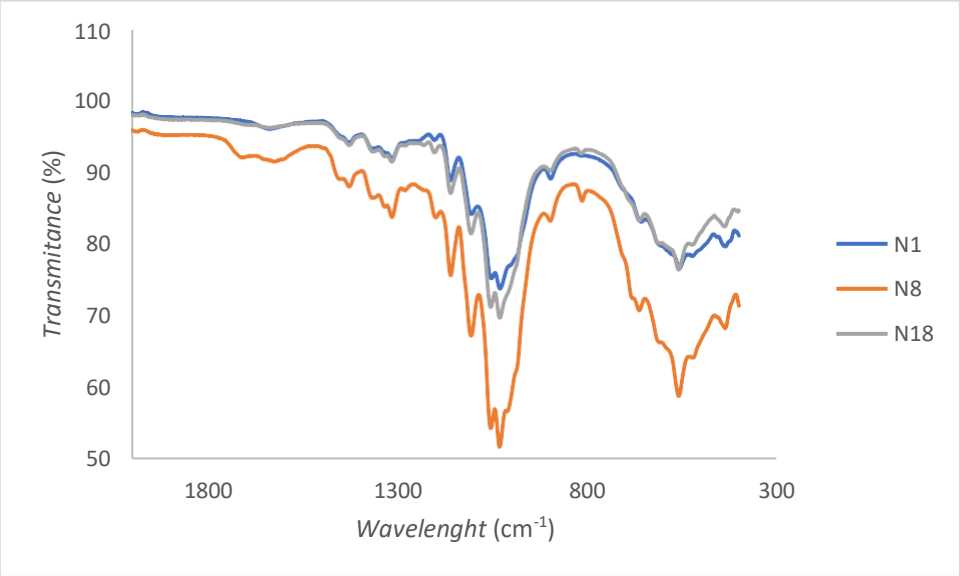

Figure 23 - FTIR spectra of N1, N8 and N18 solid residues zoomed in (1800-300 cm^{-1})

3.1.1. The effect of different temperatures on the FTIR spectra

The effect of the reaction temperature was evaluated through the comparative infrared analysis of the pair *N*(6;8). Both reactions were performed with the highest studied reaction time and catalyst amount differing only in the temperature with *N1* at 120 ºC and *N8* at 170 ºC. In Figures 24 to 26, FTIR spectra of the obtained bio-oils from *N*(6;8) are displayed.

The biggest differences seen in Figures 24 are observed at 1040, 1180, 1620, 1730 and 3350 cm^{-1}. Starting with the latter, this band is characteristic for hydroxyl groups which tend to decrease throughout the biomass conversion process so its expected a smaller band with higher temperatures which is confirmed in Figure 26. At 1620 and 1730 cm^{-1}, two bands are observed in the N8 spectra which do not appear in the *N6* spectra. This bands refer to the carbonyl group and its appearance is due to the depolymerization of cellulose which does not occur at 120 ºC (*N6* reaction temperature). The peeks observed between 1180-1040 cm^{-1} correspond to the C-O stretch deformation and its expected for a higher reaction temperature to break more C-O bonds which can be confirmed with Figure 25.

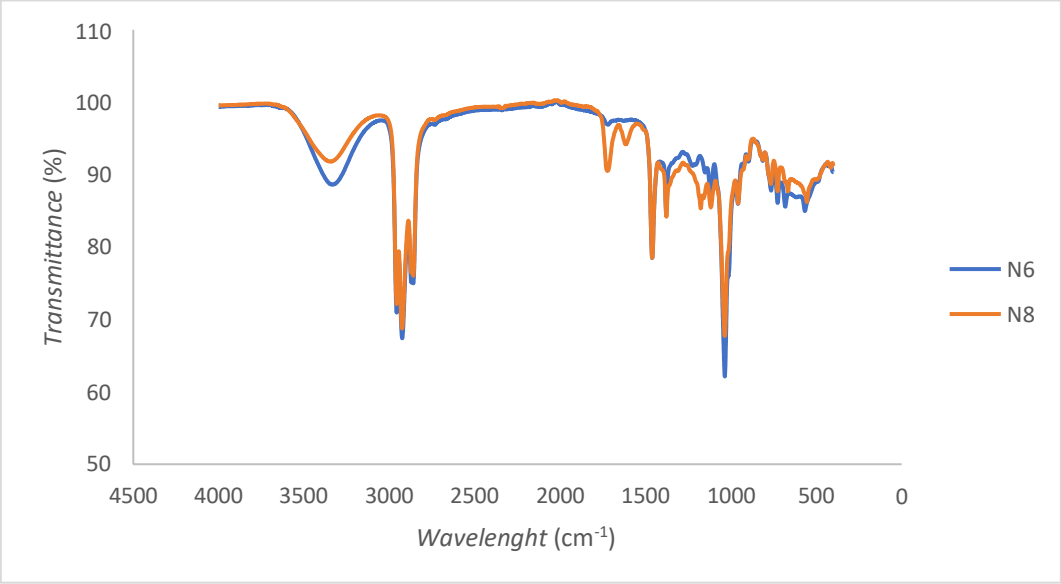

Figure 24 - FTIR spectra of N(6;8) bio-oils

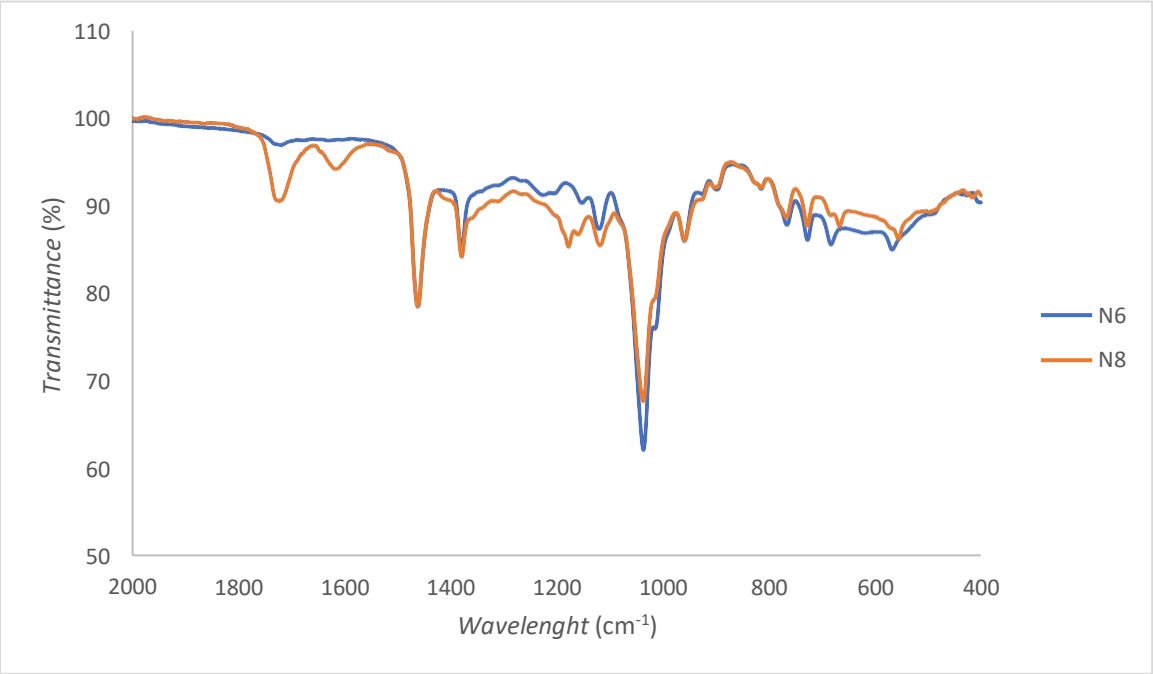

Figure 25 - FTIR spectra of N(6;8) bio-oils zoomed in (2000-400cm^{-1})

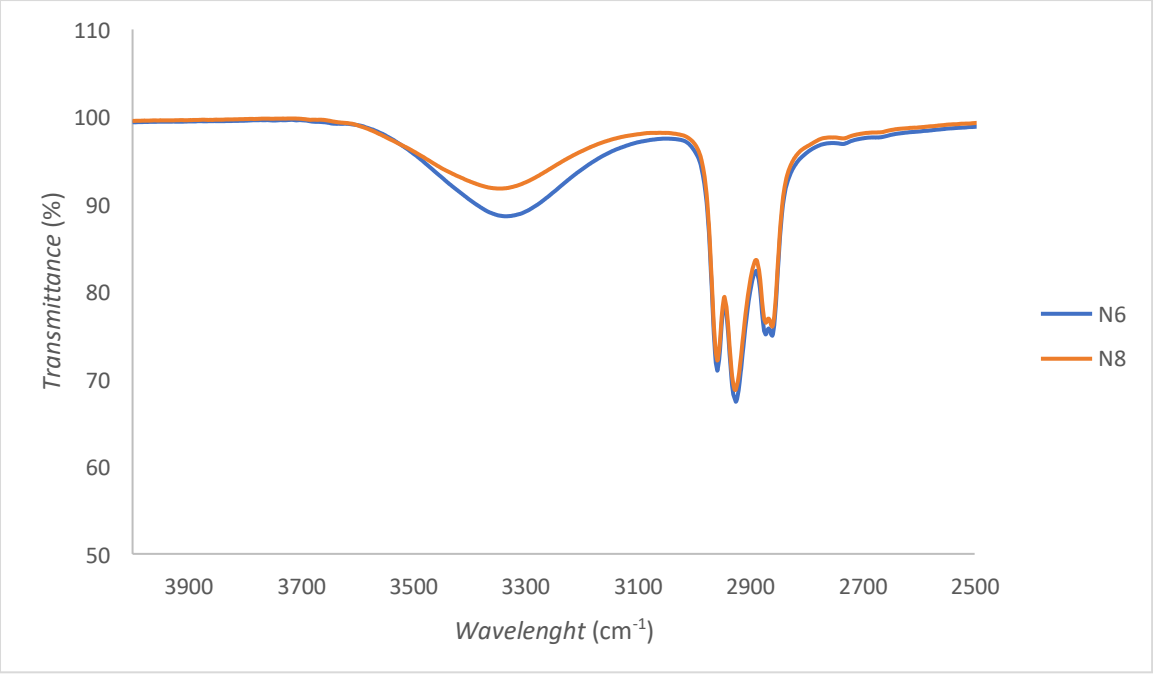

Figure 26 - FTIR spectra of N(6;8) bio-oils zoomed in (4000-2500cm^{-1})

3.1.2. The effect of different reaction times on the FTIR spectra

The effect of the reaction time was evaluated through the comparative infrared analysis of the pair *N*(7;8). Both reactions were performed with the highest studied reaction temperature and catalyst amount differing only in the reaction time with *N7* for 30 minutes and *N8* for 180 minutes. Below are displayed the FTIR spectra of the obtained bio-oils from the pair *N*(7;8).

As observed in Figures 27 and 28, the *N*(7;8) infrared spectroscopy show identical behaviour except at 1720 and 3350 cm^{-1}. The band at 3350 cm^{-1} describes a C-O stretch which is characteristic of hydroxyl groups while the band at 1720 cm^{-1} describes a C=O stretch characteristic of the carbonyl group. A higher reaction time led to a larger band at 1720 cm^{-1} and a smaller band at 3350 cm^{-1} meaning it led to a bio-oil with an higher carbonyl content and a smaller hydroxyl content.

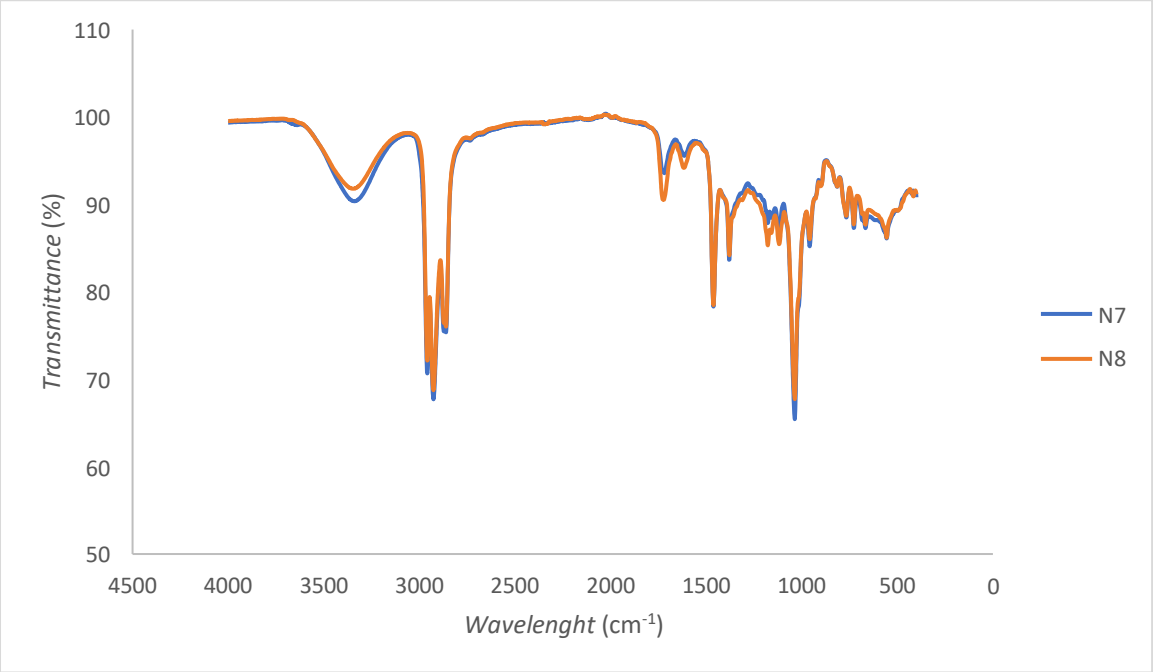

Figure 27 - FTIR spectra of N(7;8) bio-oils

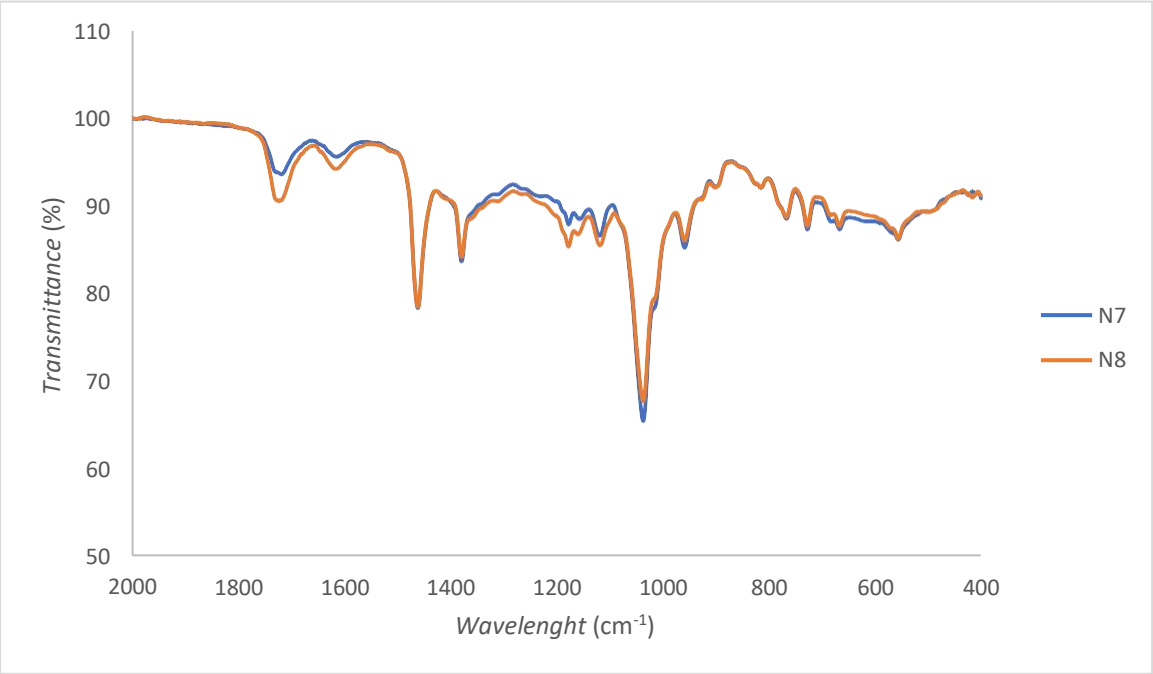

Figure 28 - FTIR spectra of N(7;8) bio-oils zoomed in (2000-400 cm^{-1})

3.1.3. The effect of different catalyst amounts on the FTIR spectra

The effect of the catalyst amount was evaluated through the comparative infrared analysis of the pair *N*(4;8). Both reactions were performed with the highest studied reaction temperature and time differing only in the amount of catalyst with *N4* with 0.5wt% and *N8* with 3wt%. Below are displayed the FTIR spectra of the obtained bio-oils from the pair *N*(4;8).

The FTIR spectra of *N*(4;8) shows differences at 1380-1110, 1700-1600 and 3350 cm^{-1}. The 3350 cm^{-1} band describes a O-H stretch characteristic of alcohols. A smaller band from *N8* means its bio-oil has a lower oxygen content. Between 1800-1700 cm^{-1}, no band is reportedin *N4*'s infrared spectroscopy unlike the *N8* spectra which shows a large band. This band describes the C=O stretch of carbonyl groups meaning the 0.5wt% catalyst amount was not enough to produce a bio-oil with carbonyl content.

So its possible to understand that an amount of catalyst equivalent to 0.5 biomass plus solvent weight percentage is not a viable operation condition.

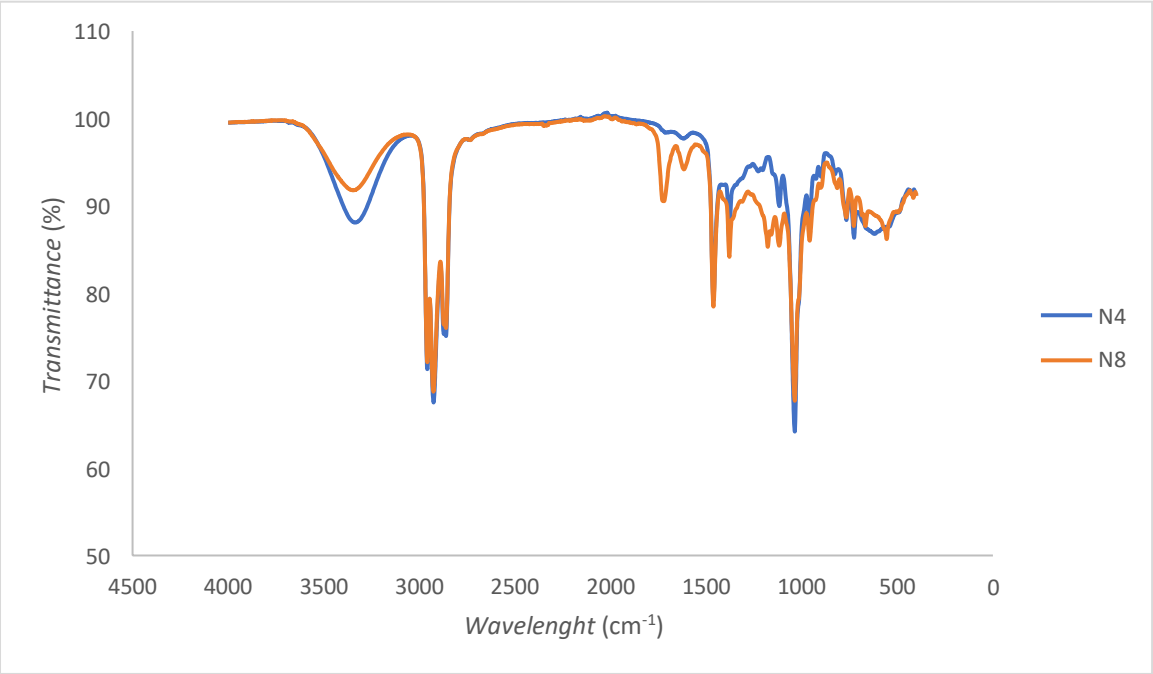

Figure 29 - FTIR spectra of N(4;8) bio-oils

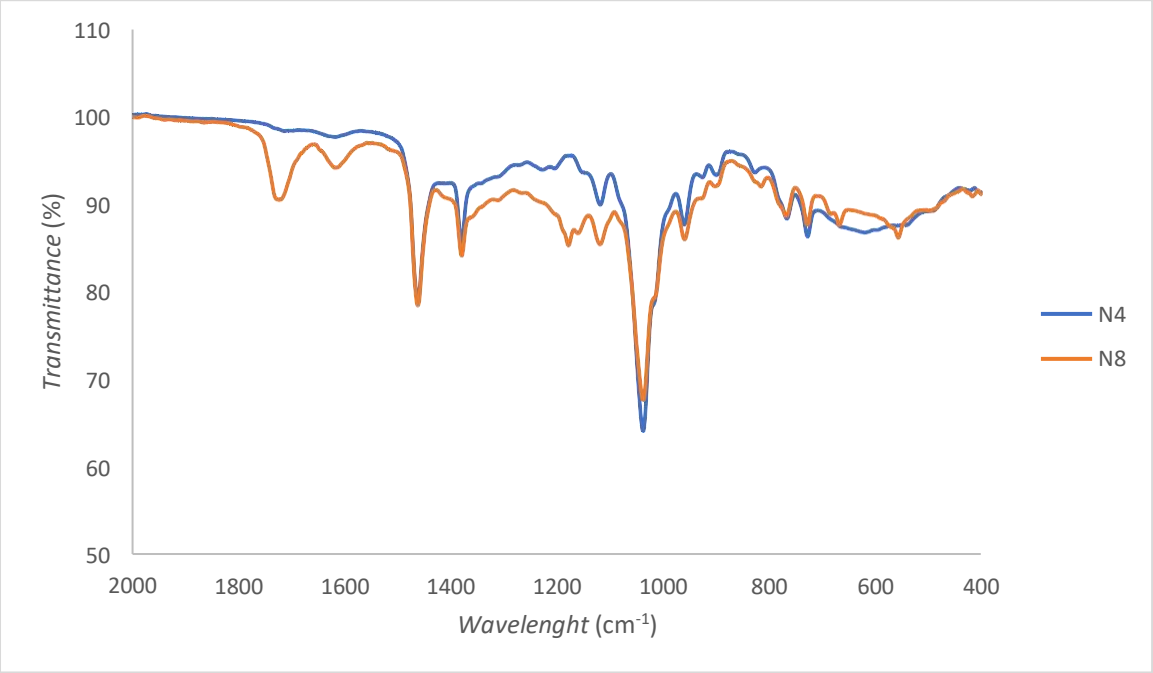

Figure 30 - FTIR spectra of N(4;8) bio-oils zoomed in (2000-400 cm^{-1})

3.2. Dynamic Viscosity Analysis

The viscosities of the *N1*, *N8* and *N18* bio-oils were evaluated at the following temperatures: 20, 25, 30, 40, 50, 60, 70 and 80 ºC. For each temperature, five viscosity tests were done for the three bio-oils. In the tables below, the average viscosity values are displayed alongside the correspondent standard deviation (SD) for each bio-oil.

Table 6 - N1 bio-oil dynamic viscosity

***T* (ºC)**	**20**	**25**	**30**	**40**	**50**	**60**	**70**	**80**
Average μ (mm^2s^{-1})	11.18	9.01	7.37	5.16	3.69	2.76	2.13	1.68
SD	0.003	0.001	0.003	0.001	0.001	0.001	0.001	0.001

Table 7 - N8 bio-oil dynamic viscosity

***T* (ºC)**	**20**	**25**	**30**	**40**	**50**	**60**	**70**	**80**
Average μ (mm^2s^{-1})	15.16	12.17	9.93	6.85	5.00	3.70	2.87	2.28
SD	0.047	0.011	0.011	0.009	0.007	0.011	0.007	0.009

Table 8 - N18 bio-oil dynamic viscosity

T (ºC)	**20**	**25**	**30**	**40**	**50**	**60**	**70**	**80**
Average μ (mm^2s^{-1})	14.08	11.26	9.12	6.24	4.45	3.30	2.52	1.97
SD	0.006	0.007	0.004	0.006	0.004	0.006	0.004	0.003

Evaluating Tables 6 to 8, its possible to verify that the bio-oils viscosity increases with the reaction time ($t_{N8} > t_{N18} > t_{N1}$) due to having more time to convert more cellulose. The obtained values also allow to conclude that the oils turn less viscous with the increase of the temperature as illustrated in Figure 31 below.

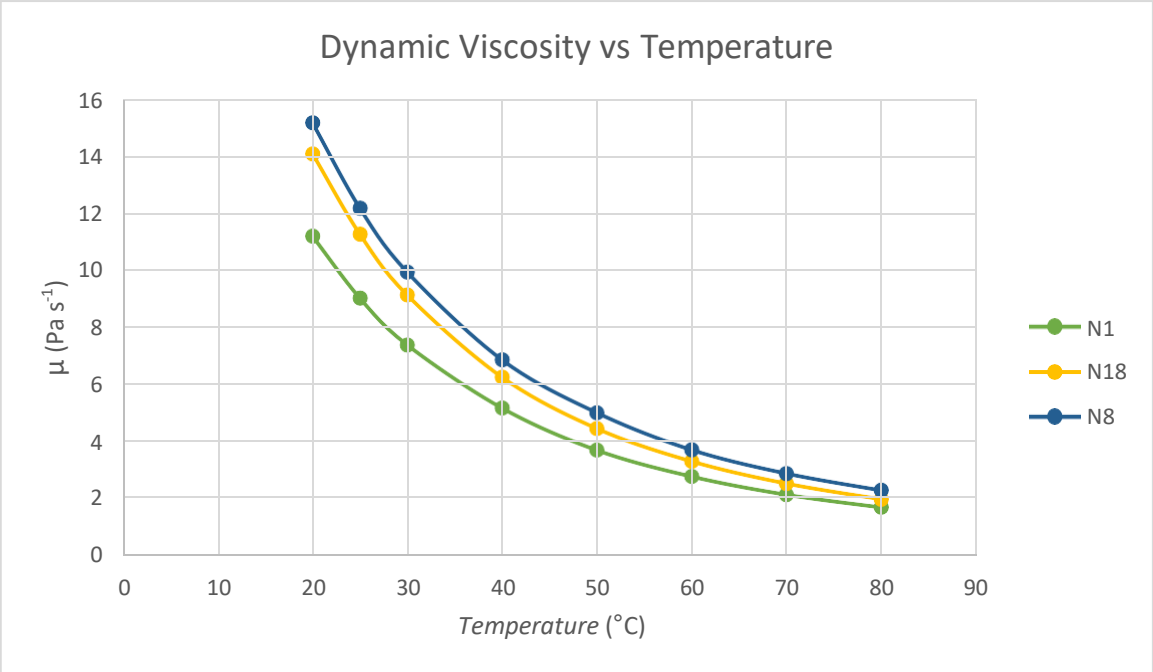

Figure 31 - Dynamic Viscosity vs Temperature

The standard deviations of Tables 6 and 7 are superior once compared to the standard deviation of Table 5. This is due to the transparency of *N1* allowing the testing with an automatic sensor while *N8* and *N18* darkest appearance blocked the sensor's ability forcing a manual count with a normal cronometer.

3.3. Density Analysis

The densities of the *N1*, *N8* and *N18* bio-oils were also evaluated at the following temperatures: 10, 20, 30, 40, 50, 60 and 70 ºC with the values for 80 ºC being extrapolated. For each temperature, 3 tests were made with the average values of density and sound velocity obtained displayed below.

Table 9 - Density and Sound Velocity of N1 bio-oil

T (ºC)	10	20	25	30	40	50	60	70	80
Density (g cm^{-3})	0.843	0.836	0.832	0.829	0.821	0.814	0.806	0.798	0.795
Sound Velocity (m s^{-1})	1372.86	1335.96	1317.85	1299.99	1264.79	1230.45	1197.22	1165.25	1128.16

Table 10 - Density and Sound Velocity of N8 bio-oil

T (ºC)	10	20	25	30	40	50	60	70	80
Density (g cm^{-3})	0.888	0.880	0.877	0.873	0.866	0.858	0.850	0.842	0.832
Sound Velocity (m s^{-1})	1384.93	1348.68	1330.95	1313.41	1278.87	1244.77	1211.27	1178.28	1142.48

Table 11 - Density and Sound Velocity of N18 bio-oil

T (ºC)	10	20	25	30	40	50	60	70	80
Density (g cm^{-3})	0.866	0.859	0.855	0.852	0.844	0.837	0.829	0.821	0.818
Sound Velocity (m s^{-1})	1380.68	1344.67	1327.04	1309.66	1275.43	1242.09	1209.06	1176.22	1140.83

The evaluation of the tables above, allows to conclude that the density of this bio-oils behaves like the viscosity, higher reaction time lead to higher densities and sound velocities (*N8 > N18 > N1*). This two properties also decrease with an increase of the testing temperature as described in Figures 32 and 33 below. This decrease could be explained with the bonding breakage promoted by higher temperatures and the consequent decrease on the average molecular weight.

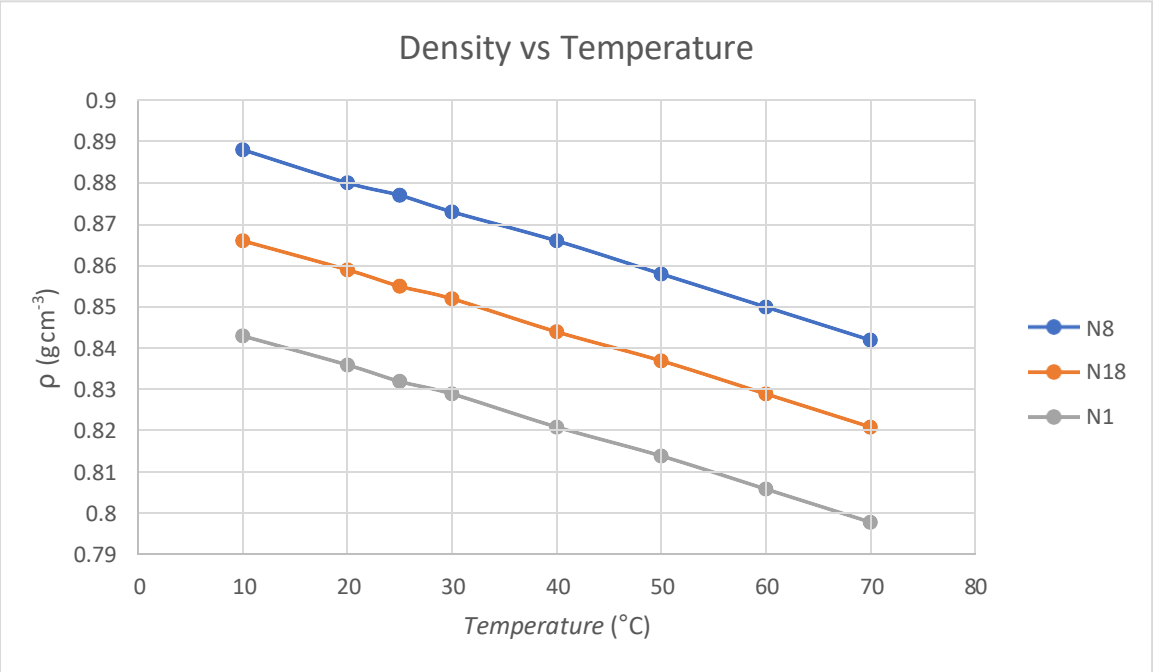

Figure 32 - Density vs Temperature

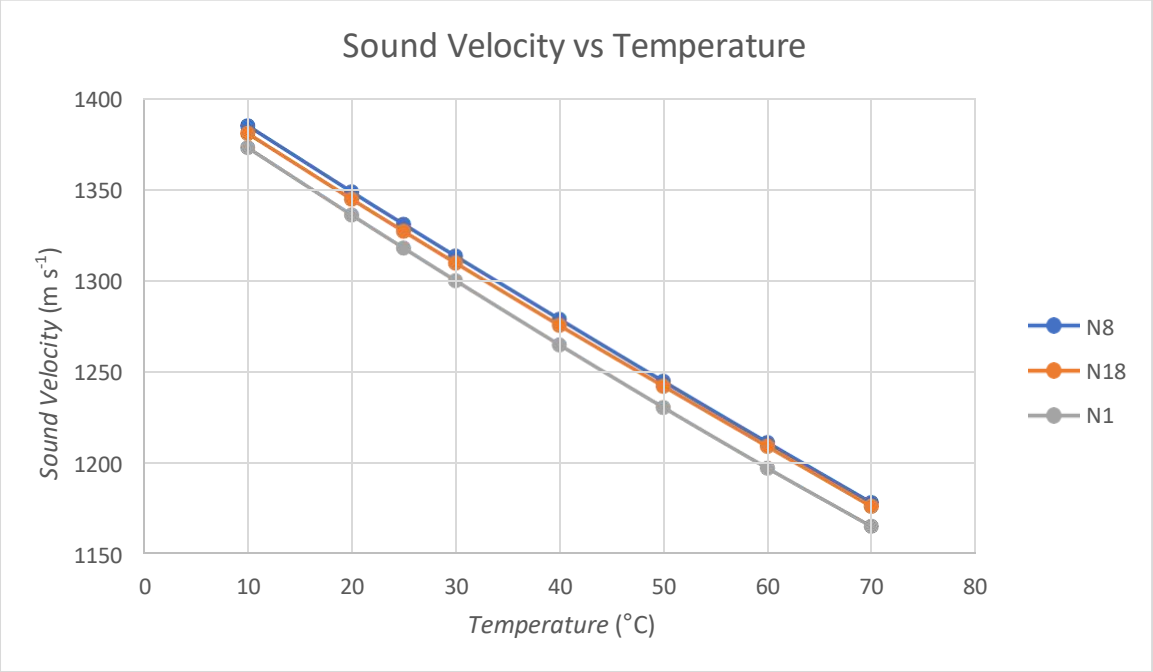

Figure 33 - Sound Velocity vs Temperature

3.4. Kinematic Viscosity Analysis

With the dynamic viscosity and the density values its possible to define the kinematic viscosity which refers to the ratio of dynamic viscosity to density as described below.

$$v = \frac{\mu}{p}$$

Based on this expression, the kinematic viscosity of *N1*, *N8* and *N18* were determined and displayed on Table 11 below.

Table 12 - Kinematic Viscosity of N1, N8 and N18 bio-oils

	20ºC	25ºC	30ºC	40ºC	50ºC	60ºC	70ºC	80ºC
N1	13.38	10.83	8.89	6.29	4.53	3.43	2.67	2.12
N8	17.23	13.87	11.37	7.91	5.83	4.35	3.41	2.74
N18	16.39	13.16	10.71	7.40	5.31	4.46	3.50	2.41

The values in Table 12 allow to conclude that the kinematic viscosity follows the same behaviour of the dynamic viscosity as its increase follows the increase of the reaction time and decreases with temperature increase as illustrated in Figure 34 below.

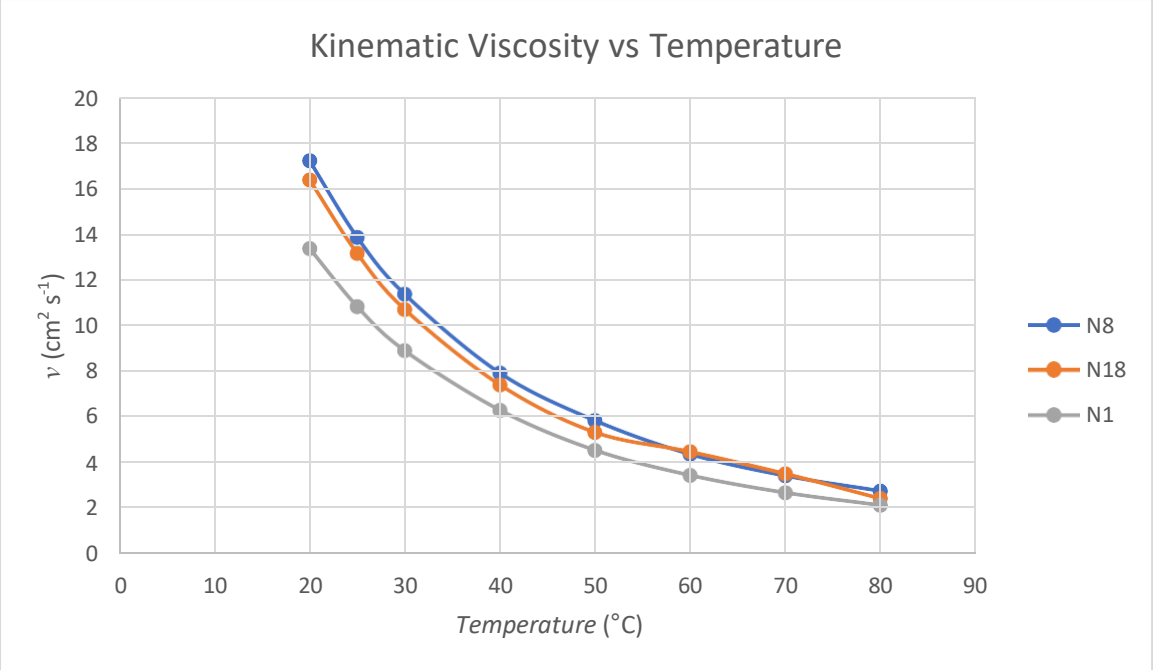

Figure 34 - Kinematic Viscosity vs Temperature

3.5. Elementar Analysis

The elementar analysis of the bio-oils and solid residues from *N1*, *N8* and *N18* were performed by LAIST (IST Analysis Laboratory). Below are represented the obtained values for each sample.

Table 13 - Bio-oils Elementar Analysis

	C (%)	H (%)	N (%)	S (%)	O (%)*
N1	67.64	13.94	< 0.5	< 2	15.92
N8	63.85	11.58	< 0.5	< 2	22.07
N18	63.01	12.05	< 0.5	< 2	22.44

Table 14 - Solid Residues Elementar Analysis

	C (%)	H (%)	N (%)	S (%)	O (%)*
N1	41.47	6.37	< 0.5	< 2	49.66
N8	48.02	6.91	< 0.5	2	42.57
N18	43.38	6.24	< 0.5	< 2	47.88

*The content of oxygen can't be directly detectable so an approximation was made by removing the other components (C,H,N and S) from the composition scale with a total of 100%**[12]**.

With this values its possible to calculate the bio-oils high heating value (HHV). The correlation used to calculate the high heating value was described by Changdong et al., with R^2 = 0.834**[37]**.

$$HHV = -1.3375 + 0.3137C + 0.7009H + 0.0318O^* \qquad (MJ\ Kg^{-1})$$

With this expression, the high heating value of the obtained bio-oils and solid residues were estimated in Table 145 below.

Table 15 - Bio-oils and solid residues HHV values

	N1 residue	***N8 residue***	***N18 residue***	***N1 oil***	***N8 oil***	***N18 oil***
HHV (MJ Kg^{-1})	17.72	19.92	18.17	30.16	27.51	27.59

The evaluated bio-oils could not reach the 40 MJ Kg^{-1} HHV mark leaving them way far from the HHV of gasoline, light fuel oil and heavy fuel oil which stand at 46.4, 44.0 and 41.8 MJ Kg^{1}, respectively**[38]**. *N1* was the lowest conversion yield but its oil showed an higher HHV value than *N8* and *N18* as seen in Table 14. This could be explained by *N1*'s reaction not forming a carbonyl group leading to a lower oxygen content and consequent higher amount of C-C bonds resulting in a higher HHV.

On the other hand, the solid residues higher heating values are all superior to the dry wood and pure cellulose HHV - 16.2 and 16.5 MJ Kg^{-1}, respectively, meaning it could be used for new liquefactions promoting a recycling process. The solid residue with the highest HHV corresponds to the reaction with the highest yield but this does not comply in the bio-oils as $HHV_{N8} < HHV_{N18} < HHV_{N1}$. Adding to a higher reaction yield, *N8* bio-oil contains more carbon and less oxygen than *N18* bio-oil so it would be expected a superior HHV. The superior HHV could be explained by the larger amount of hydrogen in *N18* bio-oil resulting in fewer C-C bonds.

4. Conclusion

In this work, the reaction media of biomass solvent liquefaction was studied through the liquefaction of paper tissue in 2-ethylhexanol with p-toluenesulfonic acid as the catalyst. The reaction time, temperature and catalyst amount were tested, with 5% being the lowest obtained yield (*N1*) and 85% the highest (*N8)*. This higher conversion was obtained working at 170 ºC for 3 hours with 3wt% of catalyst (10.8g) and its bio-oil has a density of 0.877 g dm^{-3}, a dynamic viscosity of 12.17 mm^2s^{-1} and a kinematic viscosity of 13.87 mm^2s^{-1}, at 25 ºC. All this three properties appear to decrease with the temperature increase.

The reaction set's summary fit was evaluated with MODDE® software. All four parameters - reproductibility, model validity, R2 and Q2 – exhibited values which describe a useful model – 0.993, 0.504, 0.973 and 0.896, respectively. To confirm the model's ability to predict new data, reaction *N*18 was made and its conversion yield was within the expected interval.

The reaction temperature and the catalyst concentration turned out to be the more sensitive parameters as no notable differences were reported from different tested reaction times. Regarding the temperature, a minimum of 150 ºC is required for the formation of a carbonyl group as suggested by the FTIR analysis in this work as the formation of this group was not reported below this temperature. The catalyst concentration was crucial for the conversion of cellulose but it alone is not enough to push for a high conversion yield as a high temperature is required for cellulose walls to fully disrupt.

The elementar analysis of the bio-oils and solid residues allowed to conclude that the bio-oils HHV was far to meet the fossil fuel-based oils but the solid residues showed a higher HHV than pure cellulose and dry wood inspiring the liquefaction of solid residues from previous liquefactions.

With all the above, the optimum reaction conditions are 150-200 ºC, 2-3 hours and 3wt% of catalyst.

5. Future Work

For future research is recommended to ensure that a proper agitation is being provided by the stir rod. On this work, some reactions achieved lower than expected yields which could be due to the unefficient stirring conditions that led to unreacted biomass on the reactor's wall. This work had focus on the pure cellulose liquefaction conditions but expanding this technique to other types of biomass is of great importance since the liquefaction success varies with the biomass feedstock type. Plus, other solvents and catalysts of lower price should be studied.

The results obtained in this work's elementar analysis should motivate others to study and develop the liquefaction of solid residues from previous biomass liquefactions.

After the optimization of the liquefaction parameters, its of great importance to optimize the scale-up of this process.

6. Environment and Security

When performing biomass liquefaction, some security measures are required:

- Body, hands and eyes protection throughout the entire process.
- Being a high temperature reaction, dangerous vapours are released so the liquefaction process should always be performed on a ventiladed environment like an hotte.
- When moving the reactor for the bio-oil filtration, heat resistant gloves and breathing masks must be used.
- When cleaning the laboratory material, reaction residues must be contained in a specific residue container.

On Table 16 below, the *Globally Harmonized System of Classification and Labeling of Chemicals* (GHS) of the used chemicals is displayed.

Table 16 - Global Harmonized System of Classification and Labeling of Chemicals

	Name	Hazard and Precautionary Statements	Signal Word	Pictograms
Reactant	2-ethylhexanol	H312-H315-H318-H335; P261-P280-P305+351+338	DANGER	
Catalyst	p-toluenesulfonic acid	H290-H314-H335 P280-P303 + P361 + P353-P304 + P340 + P310-P305 + P351 + P338	DANGER	
Extraction solvent	Acetone	H225-H319-H336; P210- P280-P304 + P340 + P312- P305 + P351 + P338-P337 + P313-P403 + P235	DANGER	

7. Monetary Costs

The economical weight of the project is reported below with Table 17 illustrating the cost of a single biomass liquefaction and Table 18 the cost of a single bio-oil filtration.

Table 17 - Single Liquefaction Cost

Product	Price (€)	Used weight	Cost (€)	Total (€)
2-EH	11.08 / L	300g (=361.45 mL)	4	5.42 + *x*
PTSA	47.80 / Kg	*x*	*x*	
Paper Tissue	9 / unit	0.1578 unit	1.42	

Table 18 - Single Filtration Cost

Product	Price (€)	Used	Cost (€)	Total
Acetone	1.52 / L	250 mL	0.38	0.58
Gloves	2.97 / 30 pairs	1 pair	0.09	
Filter Paper	7.71 / 100 filters	1 filter	0.08	
Syringes	3.25 / 100 units	1 unit	0.03	

On Table 18, the used weight of PTSA is described as *x* due to the variations of catalyst used throughout the work. As reported previously, the catalyst wt% used was 0.5, 1.75 and 3% with the massic values being 1.8, 6.3, and 10.8g respectively. This massic values provide the following respective catalytic costs of 0.09, 0.30 and 0.52€. With this in account, its possible to evaluate the cost of all 17 liquefactions at 97.87€.

8. References

[1] - Box, D., Wakeman, T., & Smith, J. (2005). The end of cheap oil the consequences. *Ecologist*, *35*(8), 046.

[2] - OECD (2012), OECD Environmental Outlook to 2050: The Consequences of Inaction, OECD Publishing, Paris, https://doi.org/10.1787/9789264122246-en

[3] - Vale, Mário Filipe Lima do, Lignopolyol based one-component polyurethane foams, 2015, dissertação de Mestrado em Química Tecnológica, Faculdade de Ciências da Universidade de Lisboa, https://repositorio.ul.pt/handle/10451/22347

[4] - Agency, I. E. World Energy Outlook 2011. (2011).

[5] - Vale, M., Mateus, M. M., Galhano dos Santos, R., Nieto de Castro, C., de Schrijver, A., Bordado, J. C., & Marques, A. C. (2019). Replacement of petroleum-derived diols by sustainable biopolyols in one component polyurethane foams. *Journal of Cleaner Production*, *212*, 1036–1043. https://doi.org/10.1016/j.jclepro.2018.12.088

[6] - INE, I.P./DGT, Estatísticas de Uso e Ocupação do Solo – 2018

[7] - Vanholme, B. et al. Towards a carbon-negative sustainable bio-based economy. Front. Plant Sci. 4, 1–17 (2013)

[8] - Singh, R., Krishna, B. B., Mishra, G., Kumar, J., & Bhaskar, T. (2016). Strategies for selection of thermo-chemical processes for the valorisation of biomass. *Renewable Energy*, *98*, 226–237. https://doi.org/10.1016/j.renene.2016.03.023

[9] - Pan, H. (2011). Synthesis of polymers from organic solvent liquefied biomass: A review. *Renewable and Sustainable Energy Reviews*, *15*(7), 3454–3463. https://doi.org/10.1016/j.rser.2011.05.002

[10] - Zhou, C. H., Xia, X., Lin, C. X., Tong, D. S., & Beltramini, J. (2011). Catalytic conversion of lignocellulosic biomass to fine chemicals and fuels. *Chemical Society Reviews*, *40*(11), 5588–5617. https://doi.org/10.1039/c1cs15124j

[11] - Durak, H. (2019). Characterization of products obtained from hydrothermal liquefaction of biomass (Anchusa azurea) compared to other thermochemical conversion methods. *Biomass Conversion and Biorefinery*, *9*(2), 459–470. https://doi.org/10.1007/s13399-019-00379-4

[12] - Dimitriadis, A., & Bezergianni, S. (2017). Hydrothermal liquefaction of various biomass and waste feedstocks for biocrude production: A state of the art review. *Renewable and Sustainable Energy Reviews*, *68*(September 2015), 113–125. https://doi.org/10.1016/j.rser.2016.09.120

[13] - Mateus, M. M., Bordado, J. C., & Dos Santos, R. G. (2016). Potential biofuel from liquefied cork - Higher heating value comparison. *Fuel*, *174*, 114–117. https://doi.org/10.1016/j.fuel.2016.01.081

[14] - Li, C., & Zhao, Z. K. (2007). Efficient acid-catalyzed hydrolysis of cellulose in ionic liquid. *Advanced Synthesis and Catalysis*, *349*(11–12), 1847–1850. https://doi.org/10.1002/adsc.200700259

[15] - Silva, S. P. et al. Cork : properties, capabilities and applications. Int. Mater. Rev. 50, 345–365 (2005).

[16] - Kim, J. Y., Lee, H. W., Lee, S. M., Jae, J., & Park, Y. K. (2019). Overview of the recent advances in lignocellulose liquefaction for producing biofuels, bio-based materials and chemicals. *Bioresource Technology*, *279*(January), 373–384. https://doi.org/10.1016/j.biortech.2019.01.055

[17] - Brandt, A., Gräsvik, J., Hallett, J. P. & Welton, T. Deconstruction of lignocellulosic biomass with ionic liquids. Green Chem. 15, 550–583 (2013)

[18] - Khatib, H. (2012). IEA World Energy Outlook 2011-A comment. *Energy Policy*, *48*, 737–743. https://doi.org/10.1016/j.enpol.2012.06.007

[19] - Condeço, J. A. D., Hariharakrishnan, S., Ofili, O. M., Mateus, M. M., Bordado, J. M., & Correia, M. J. N. (2021). Energetic valorisation of agricultural residues by solvent-based liquefaction. *Biomass and Bioenergy*, *147*(January). https://doi.org/10.1016/j.biombioe.2021.106003

[20] - Nelson, D. A., Molton, P. M., Russell, J. A., & Hallen, R. T. (1984). Application of Direct Thermal Liquefaction for the Conversion of Cellulosic Biomass. *Industrial and Engineering Chemistry Product Research and Development*, *23*(3), 471–475. https://doi.org/10.1021/i300015a029

[21] - Mateus, M. M., Gaspar, D., Matos, S., Rego, A., Motta, C., Castanheira, I., Bordado, J. M., & Galhano Dos Santos, R. (2019). Converting a residue from an edible source (Ceratonia siliqua L.) into a bio-oil. *Journal of Environmental Chemical Engineering*, *7*(2), 103004. https://doi.org/10.1016/j.jece.2019.103004

[22] - Yang, Z., Peng, H., Wang, W., & Liu, T. (2010). Crystallization behavior of poly(ε-caprolactone)/layered double hydroxide nanocomposites. *Journal of Applied Polymer Science*, *116*(5), 2658–2667. https://doi.org/10.1002/app

[23] - Wu, X. F., Zhang, J. J., Huang, Y. H., Li, M. F., Bian, J., & Peng, F. (2019). Comparative investigation on bio-oil production from eucalyptus via liquefaction in subcritical water and supercritical ethanol. *Industrial Crops and Products*, *140*(July), 111695. https://doi.org/10.1016/j.indcrop.2019.111695

[24] - Wu, H., Chen, F., Liu, M., & Wang, J. (2017). Preparation of microcrystalline cellulose by liquefaction of eucalyptus sawdust in ethylene glycol catalyzed by acidic ionic liquid. *BioResources*, *12*(2), 3766–3777. https://doi.org/10.15376/biores.12.2.3766-3777

[25] - Zou, X., Qin, T., Huang, L., Zhang, X., Yang, Z., & Wang, Y. (2009). Mechanisms and main regularities of biomass liquefaction with alcoholic solvents. *Energy and Fuels*, *23*(10), 5213–5218. https://doi.org/10.1021/ef900590b

[26] - Xu, J., Zhai, Q., Xie, X., Jiang, J., & Shupe, T. F. (2020). Valorization of Bamboo Biomass by Selective Liquefaction Reaction for the Production of Sugar and Phenolic Platform

Chemicals. *Energy and Fuels*, *34*(6), 7131–7139. https://doi.org/10.1021/acs.energyfuels.0c00875

[27] - Mun, S. P., Hassan, E. B. M., & Yoon, T. H. (2001). Evaluation of organic sulfonic acids as catalyst during cellulose liquefaction using ethylene carbonate. In *Journal of Industrial and Engineering Chemistry* (Vol. 7, Issue 6, pp. 430–434).

[28] – Xu, J., Xie, X., Wang, J., & Jiang, J. (2016). Directional liquefaction coupling fractionation of lignocellulosic biomass for platform chemicals. *Green Chemistry*, *18*(10), 3124–3138. https://doi.org/10.1039/c5gc03070f

[29] - Galhano dos Santos, R., Ventura, P., Bordado, J. C., & Mateus, M. M. (2017). Direct and efficient liquefaction of potato peel into bio-oil. *Environmental Chemistry Letters*, *15*(3), 453–458. https://doi.org/10.1007/s10311-017-0620-8

[30] - Hu, S., Luo, X. & Li, Y. Polyols and polyurethanes from the liquefaction of lignocellulosic biomass. ChemSusChem 7, 66–72 (2014)

[31] - H. Zhang, H. Pang, J. Shi, T. Fu, B. Liao, Investigation of liquefied wood residues based on cellulose, hemicellulose and lignin, J. Appl. Sci. 123 (2012) 378–386

[32] - Braz, A., Mateus, M. M., Santos, R. G. dos, Machado, R., Bordado, J. M., & Correia, M. J. N. (2019). Modelling of pine wood sawdust thermochemical liquefaction. *Biomass and Bioenergy*, *120*(April 2018), 200–210. https://doi.org/10.1016/j.biombioe.2018.11.001

[33] - Pan, Z. qian, Huang, H. jun, Zhou, C. fei, Xiao, X. feng, He, X. wu, Lai, F. ying, & Xiong, J. bo. (2018). Highly efficient conversion of camphor tree sawdust into bio-oil and biochar products by liquefaction in ethanol-water cosolvent. *Journal of Analytical and Applied Pyrolysis*, 186–198. https://doi.org/10.1016/j.jaap.2018.10.006

[34] - Rinaldi, R., Meine, N., vom Stein, J., Palkovits, R., & Schüth, F. (2010). Which controls the depolymerization of cellulose in ionic liquids: The solid acid catalyst or cellulose? *ChemSusChem*, *3*(2), 266–276. https://doi.org/10.1002/cssc.200900281

[35] - Juhaida MF, Paridah MT, Hilmi MM, Sarani Z, Jalaluddin H, Zaki ARM. Liquefaction of kenaf core for wood laminating adhesive. Bioresour Technol 2010;101:1355–60

[36] - Zhai, Q., Li, F., Wang, F. *et al.* Liquefaction of poplar biomass for value-added platform chemicals. *Cellulose* **25,** 4663–4675 (2018). https://doi.org/10.1007/s10570-018-1872-6

[37] – Sheng, C., & Azevedo, J. L. T. Ã. (2005). *Estimating the higher heating value of biomass fuels from basic analysis data*. *28*, 499–507. https://doi.org/10.1016/j.biombioe.2004.11.008

[38] - Engineering ToolBox, (2003). Fuels - Higher and Lower Calorific Values.

Appendix

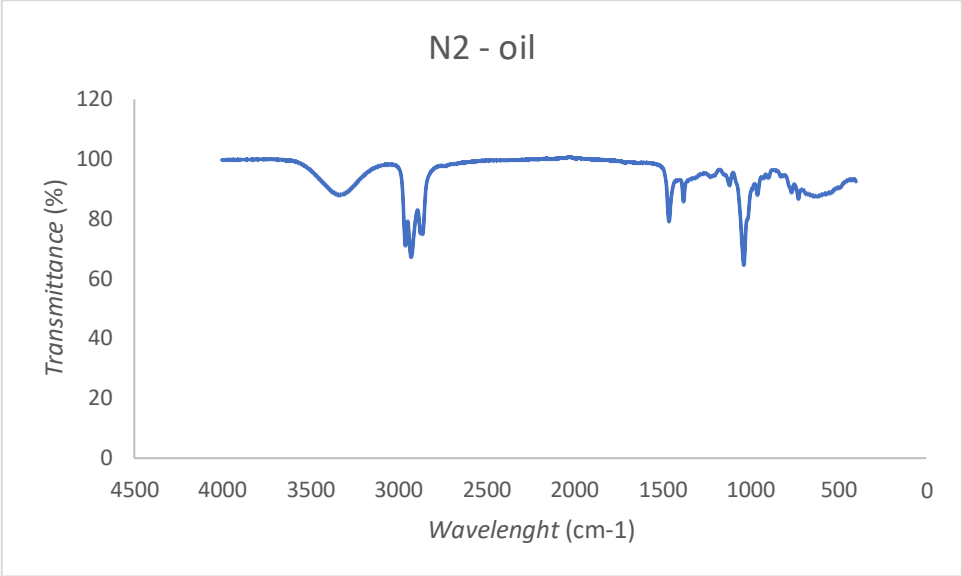

Figure 35 - N2 bio-oil FTIR

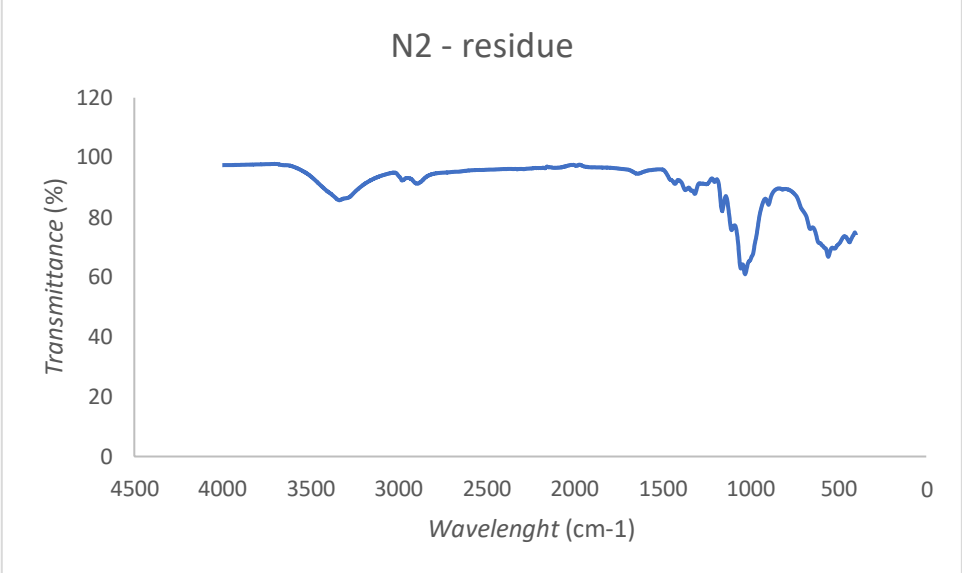

Figure 36 - N2 solid residue FTIR

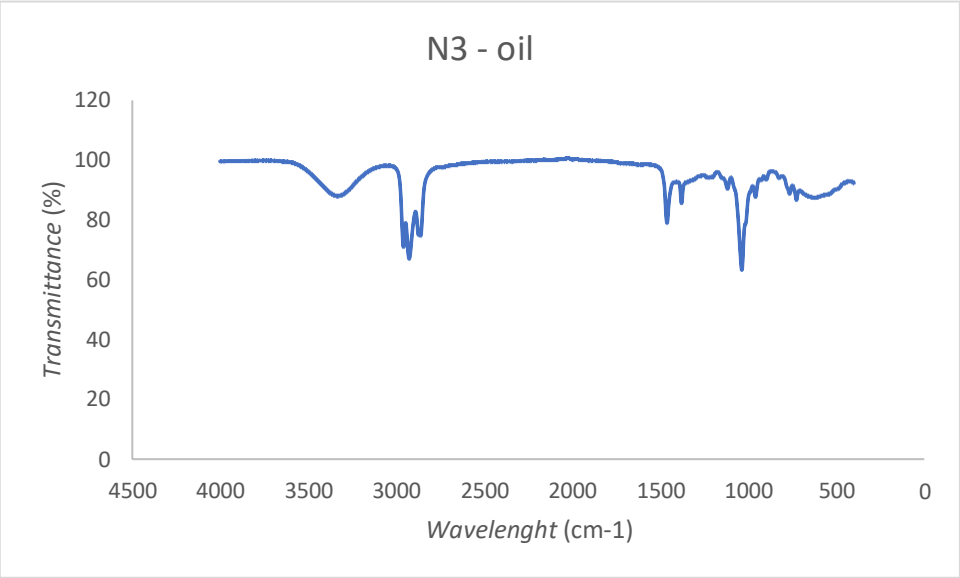

Figure 37 - N3 bio-oil FTIR

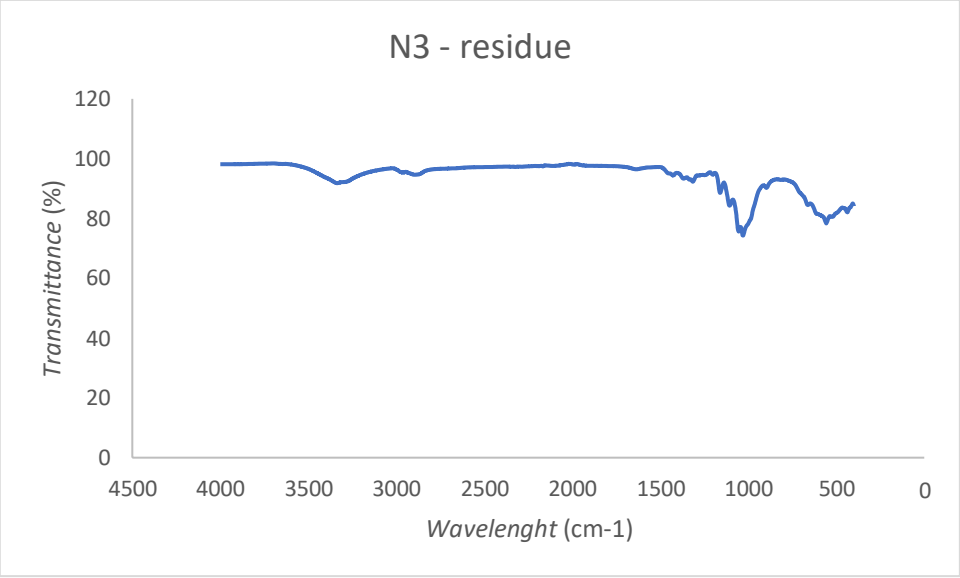

Figure 38 - N3 solid residue FTIR

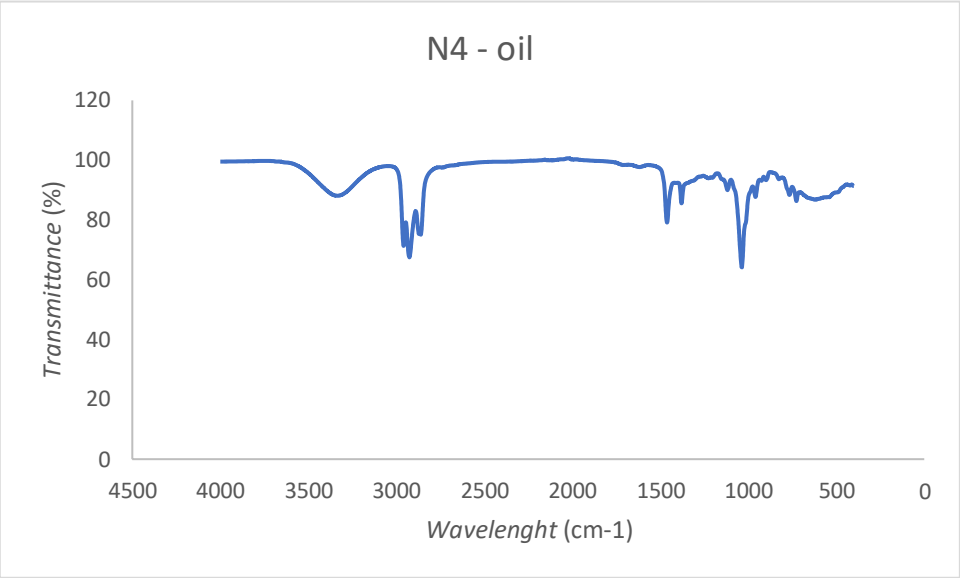

Figure 39 - N4 bio-oil FTIR

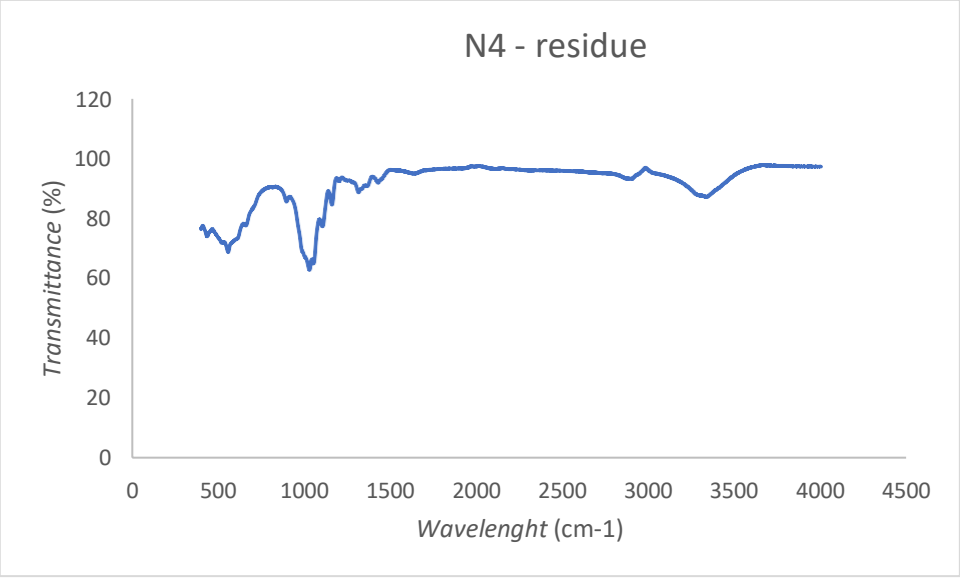

Figure 40 - N4 solid residue FTIR

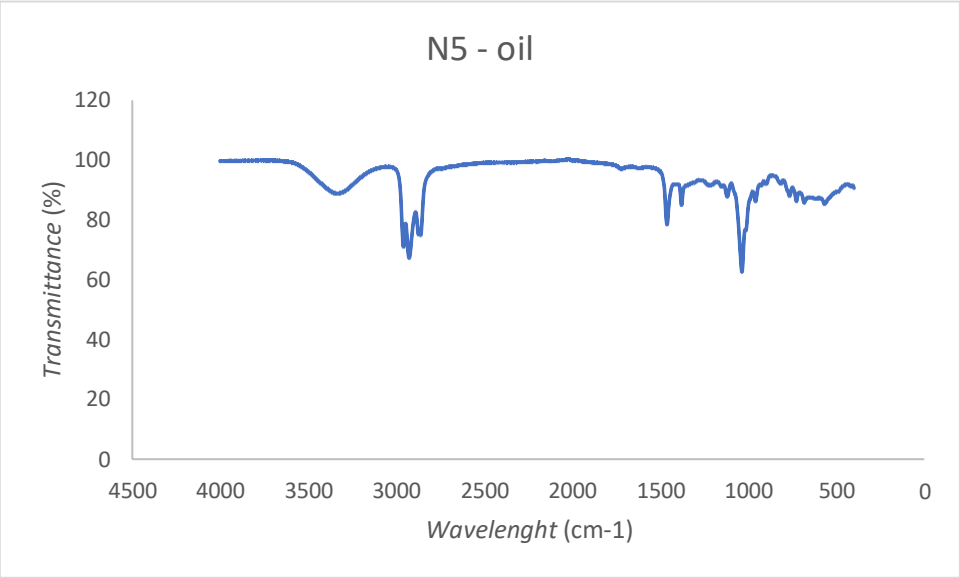

Figure 41 - N5 bio-oil FTIR

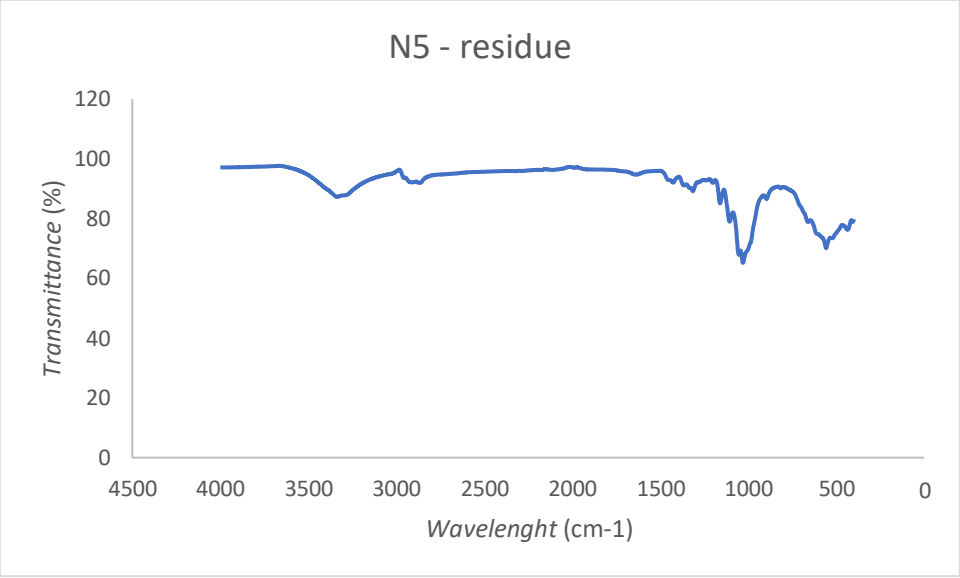

Figure 42 - N5 solid residue FTIR

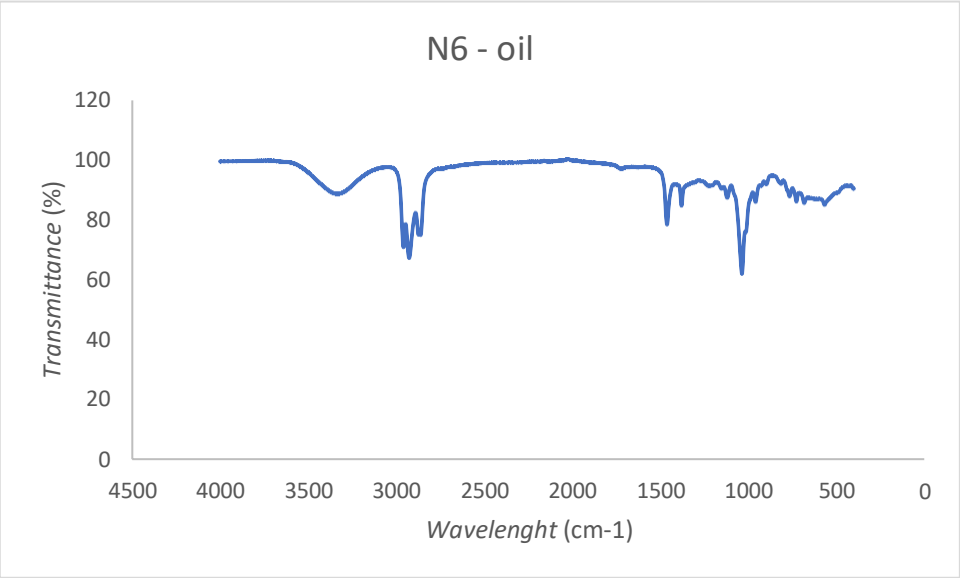

Figure 43 - N6 bio-oil FTIR

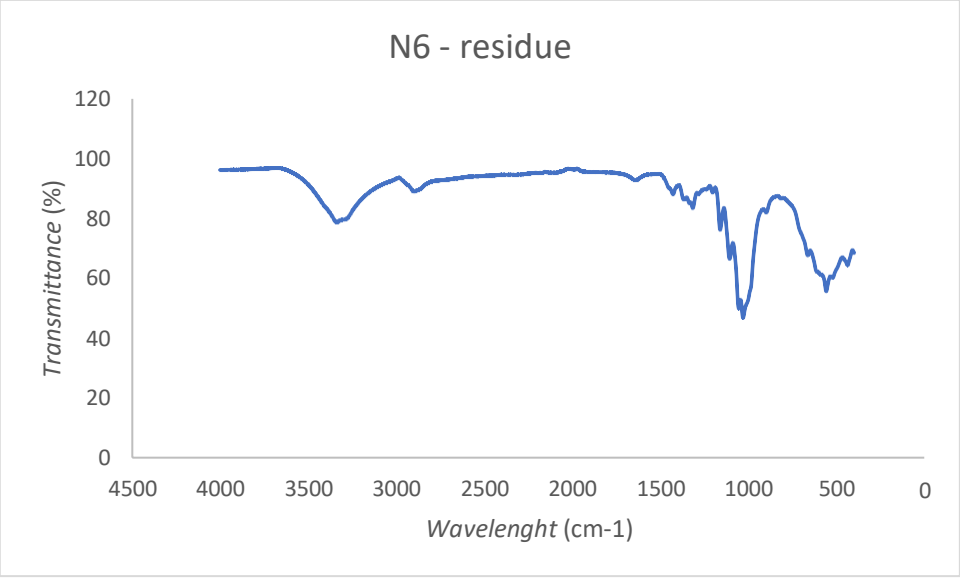

Figure 44 - N6 solid residue FTIR

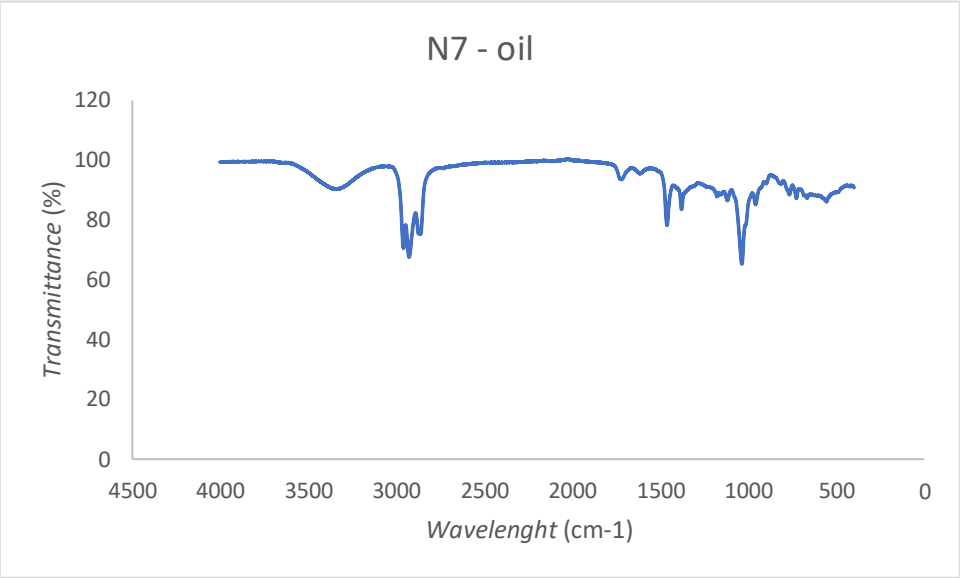

Figure 45 - N7 bio-oil FTIR

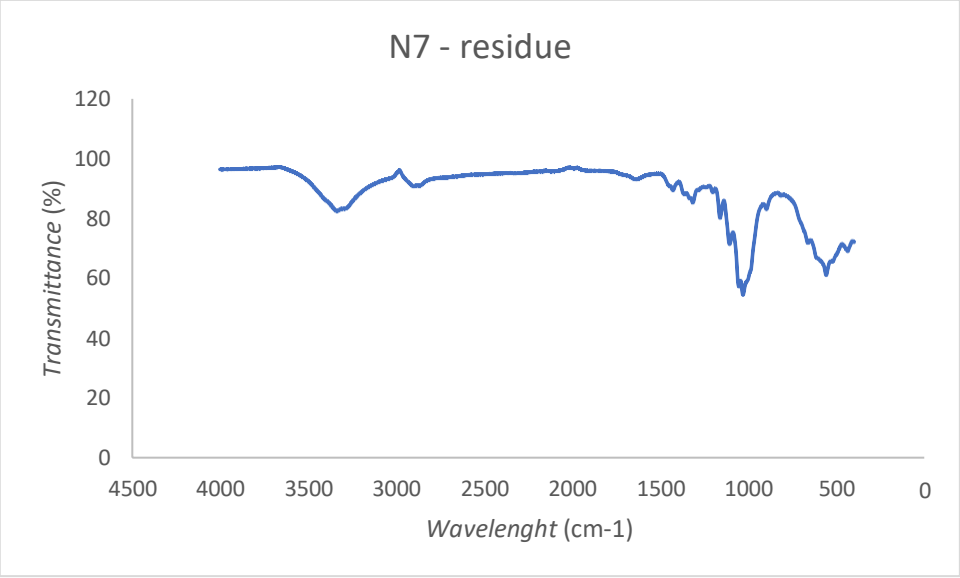

Figure 46 - N7 solid residue FTIR

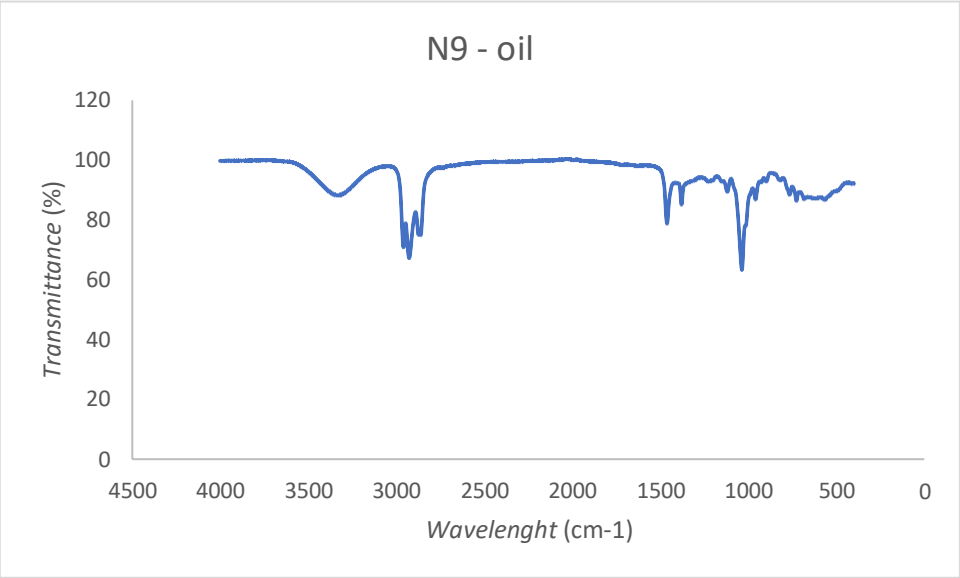

Figure 47 - N9 bio-oil FTIR

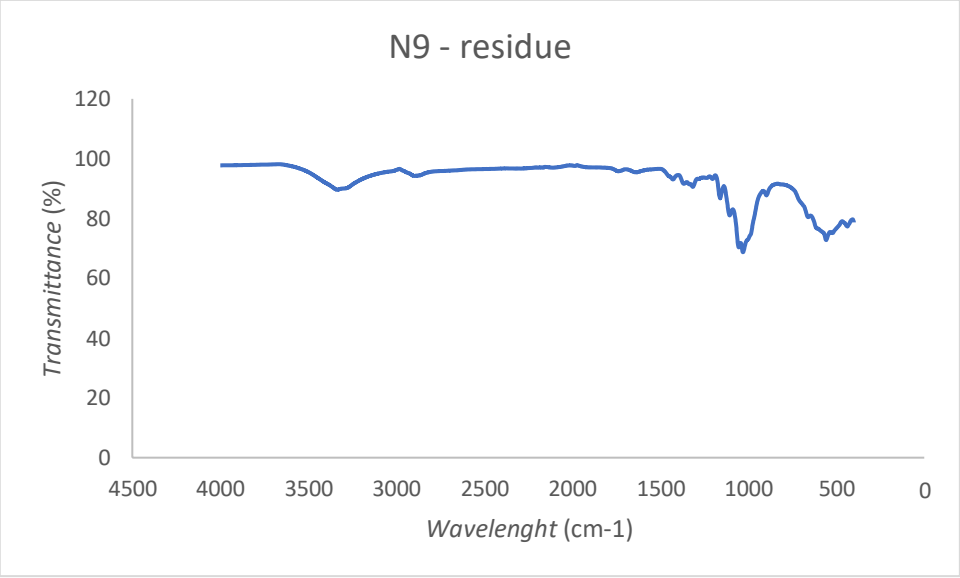

Figure 48 - N9 solid residue FTIR

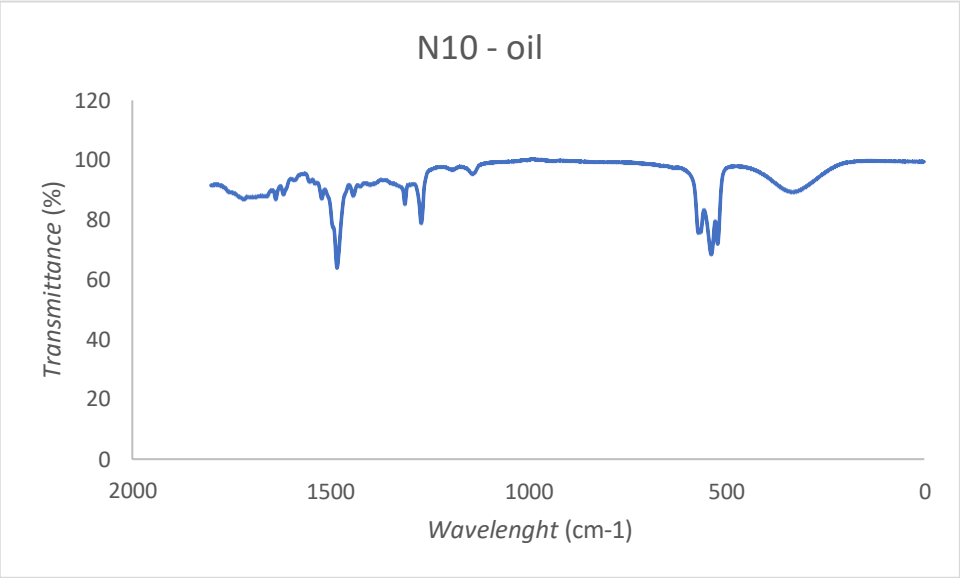

Figure 49 - N10 bio-oil FTIR

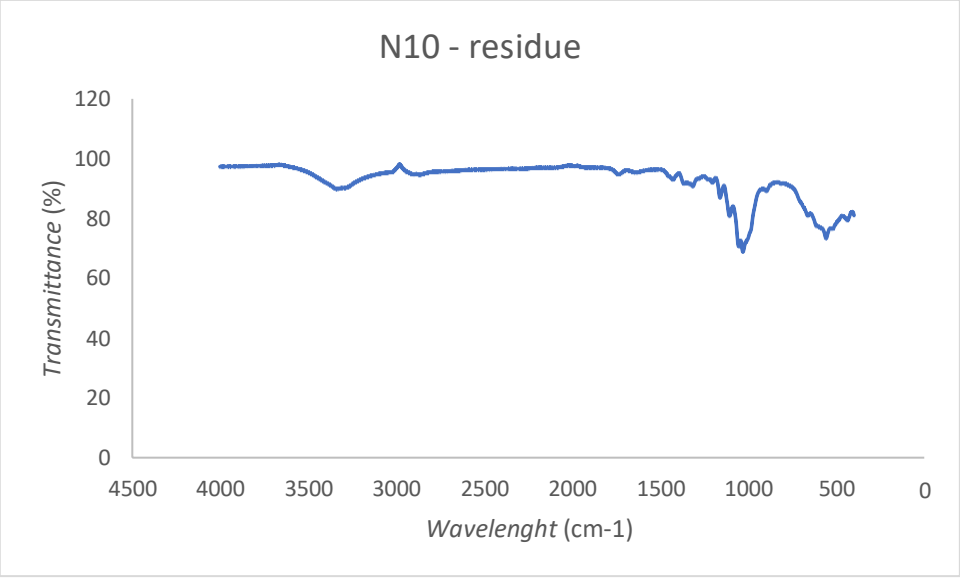

Figure 50 - N10 solid residue FTIR

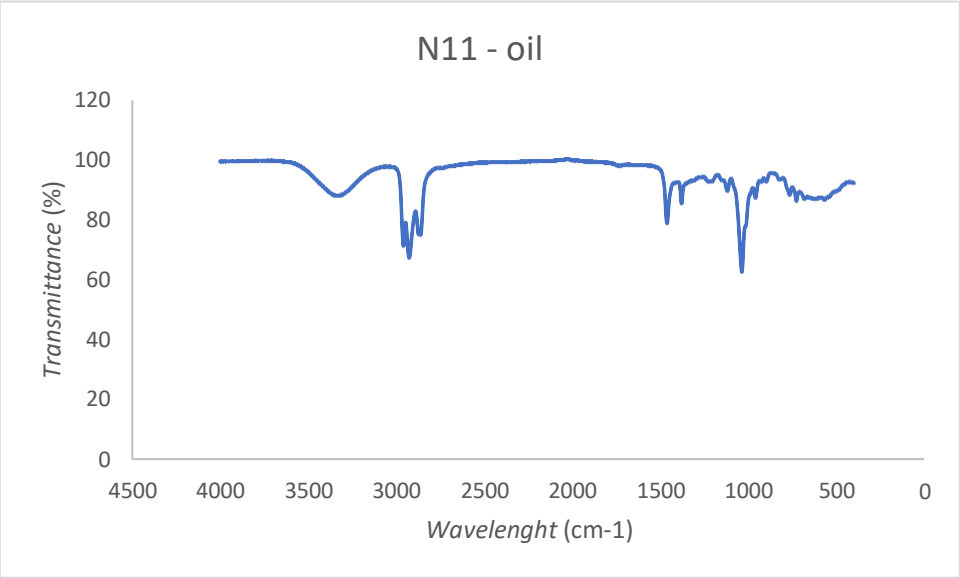

Figure 51 - N11 bio-oil FTIR

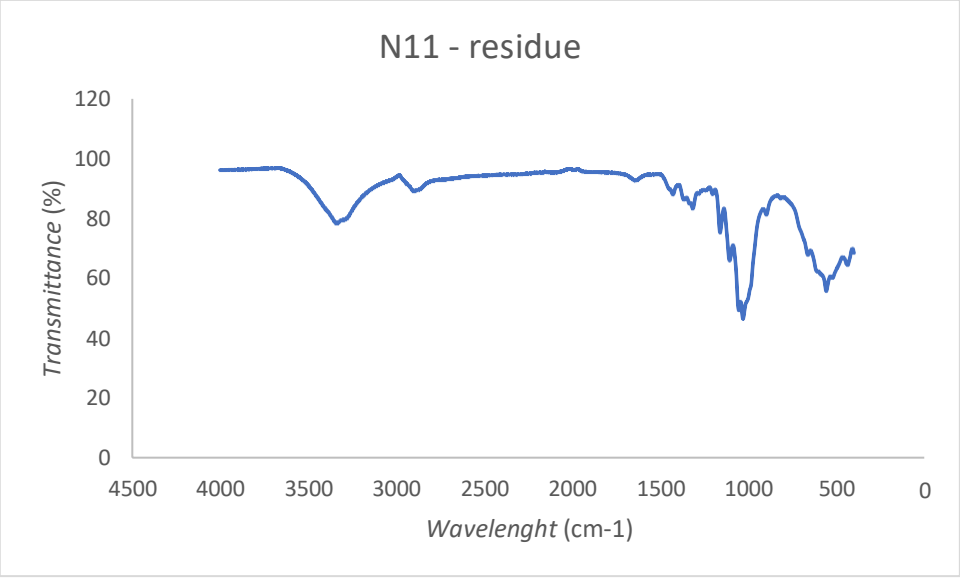

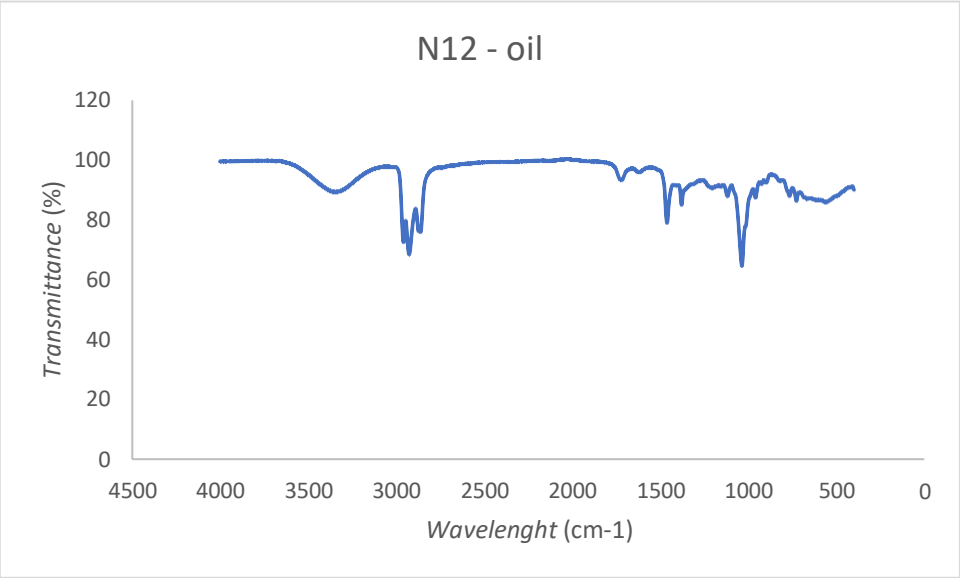

Figure 52 - N12 bio-oil FTIR

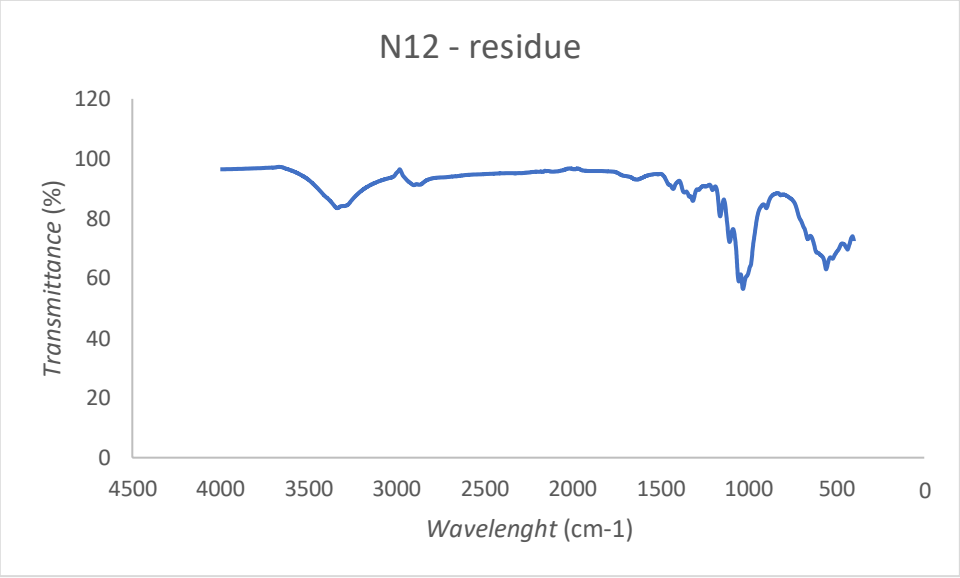

Figure 53 - N12 solid residue FTIR

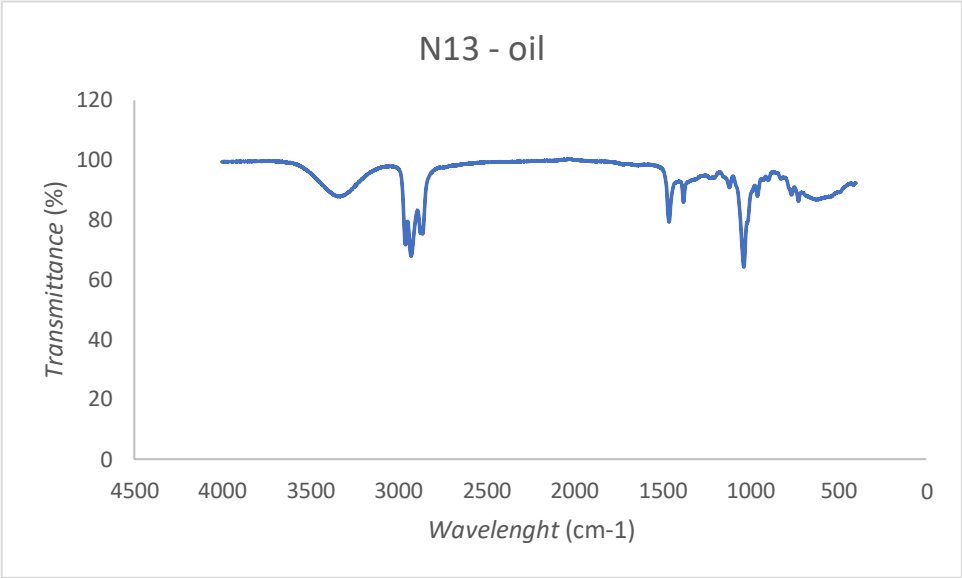

Figure 54 - N13 bio-oil FTIR

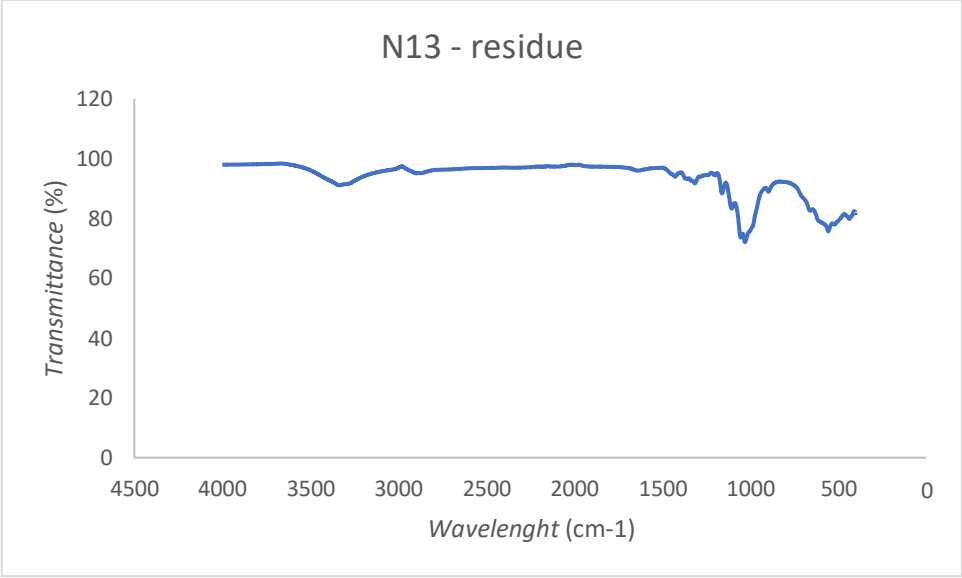

Figure 55 - N13 solid residue FTIR

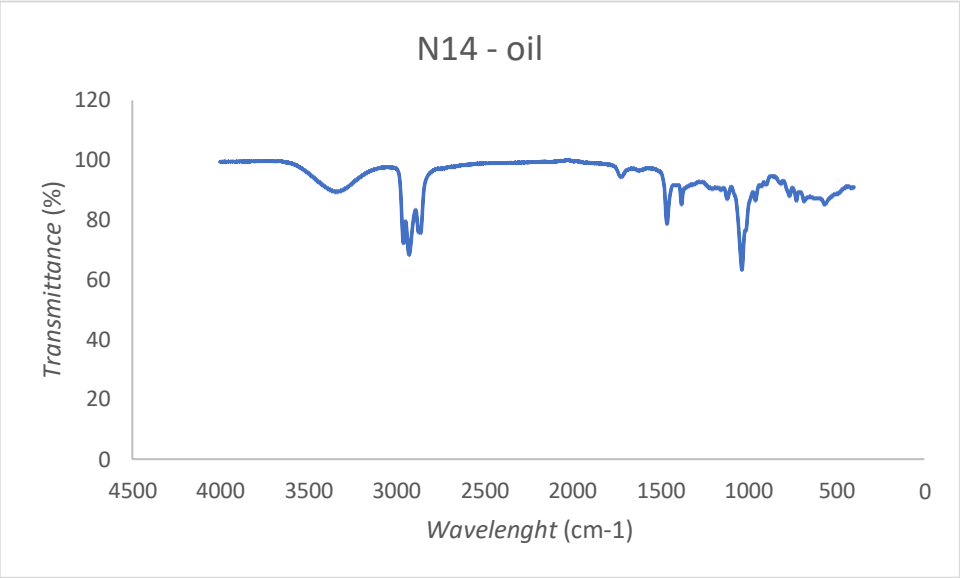

Figure 56 - N14 bio-oil FTIR

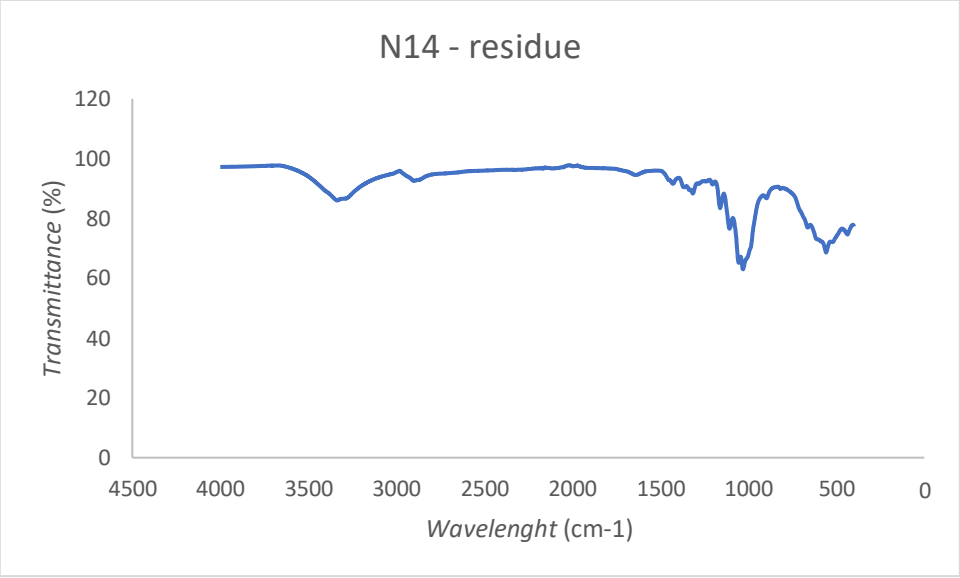

Figure 57 - N14 solid residue FTIR

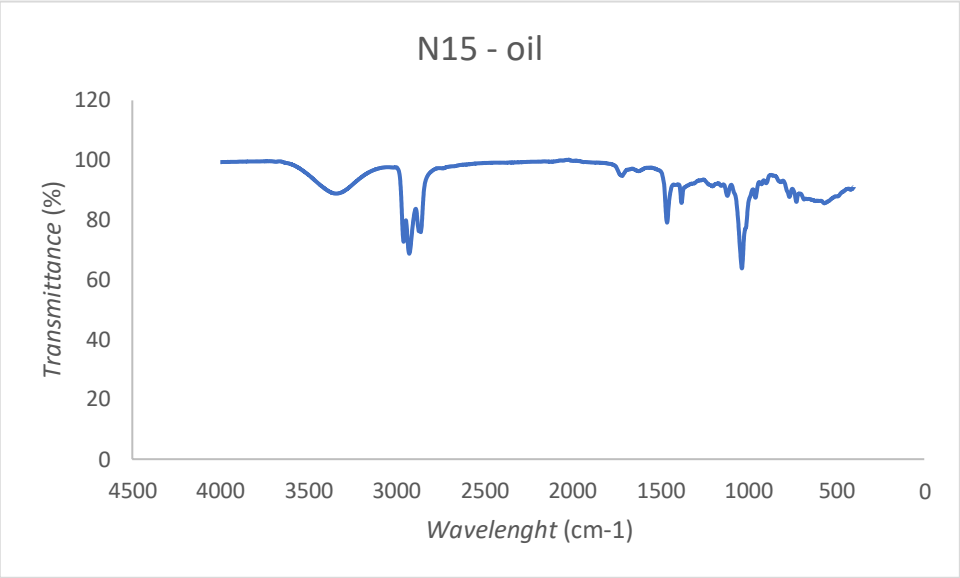

Figure 58 - N15 bio-oil FTIR

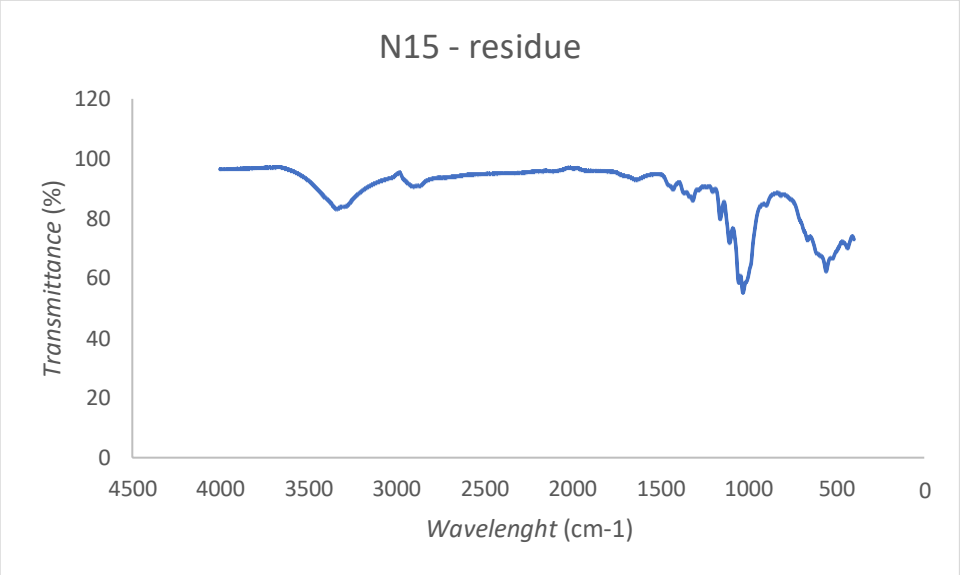

Figure 59 - N15 solid residue FTIR

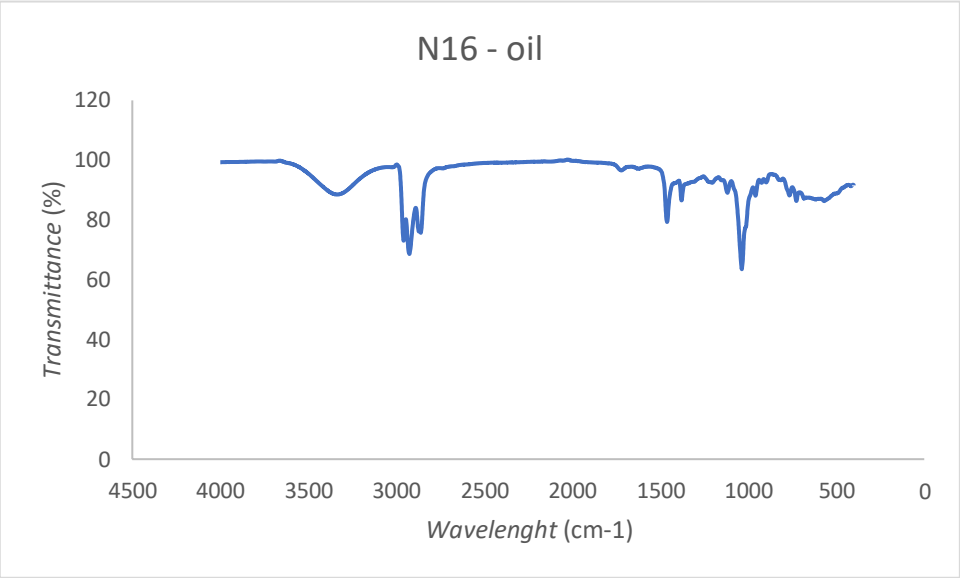

Figure 60 - N16 bio-oil FTIR

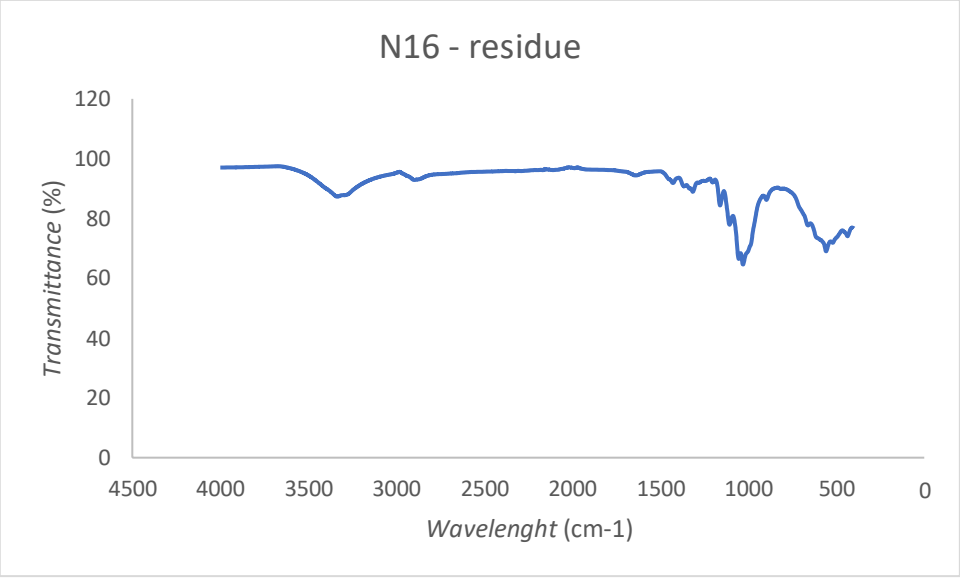

Figure 61 - N16 solid residue FTIR

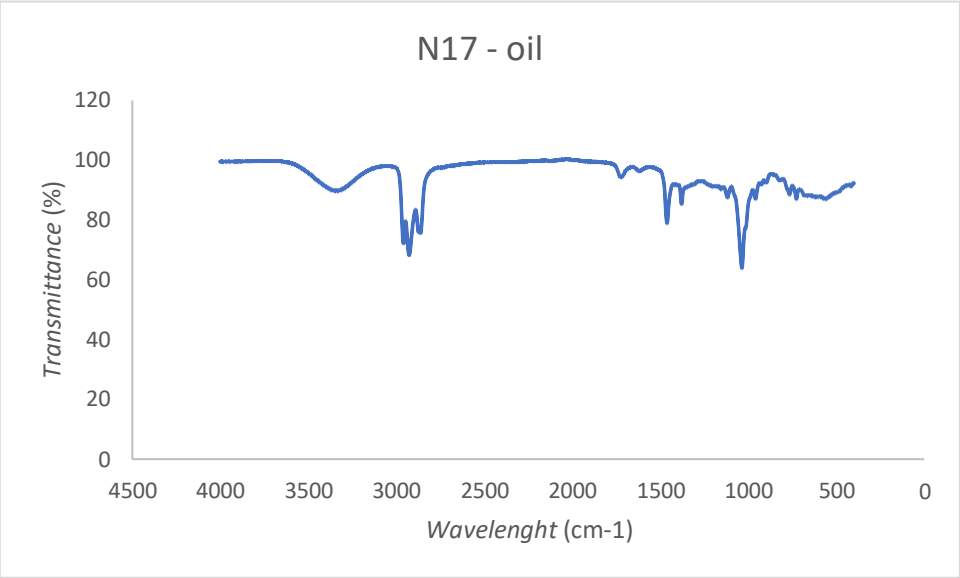

Figure 62 - N17 bio-oil FTIR

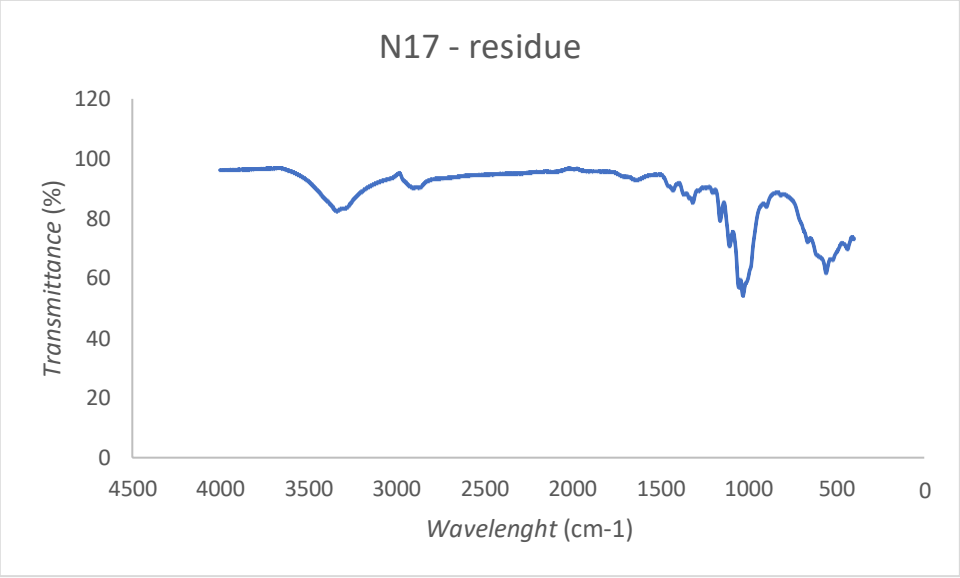

Figure 63 - N17 solid residue FTIR

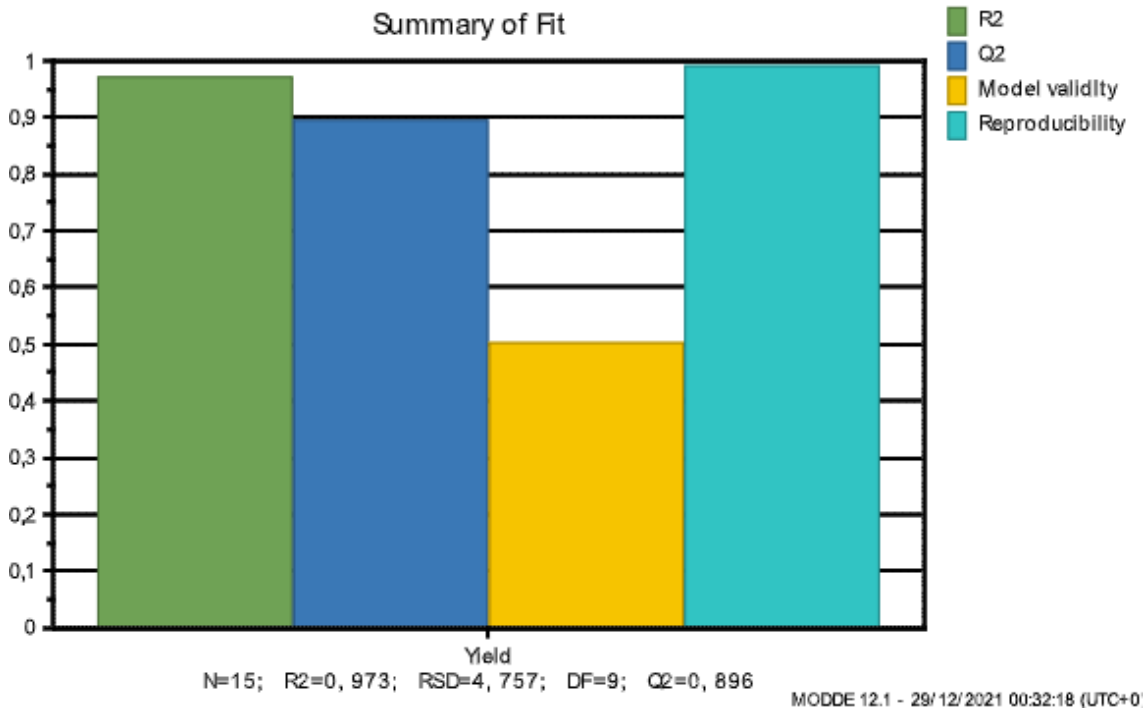

Figure 64 - Model Summary of Fit

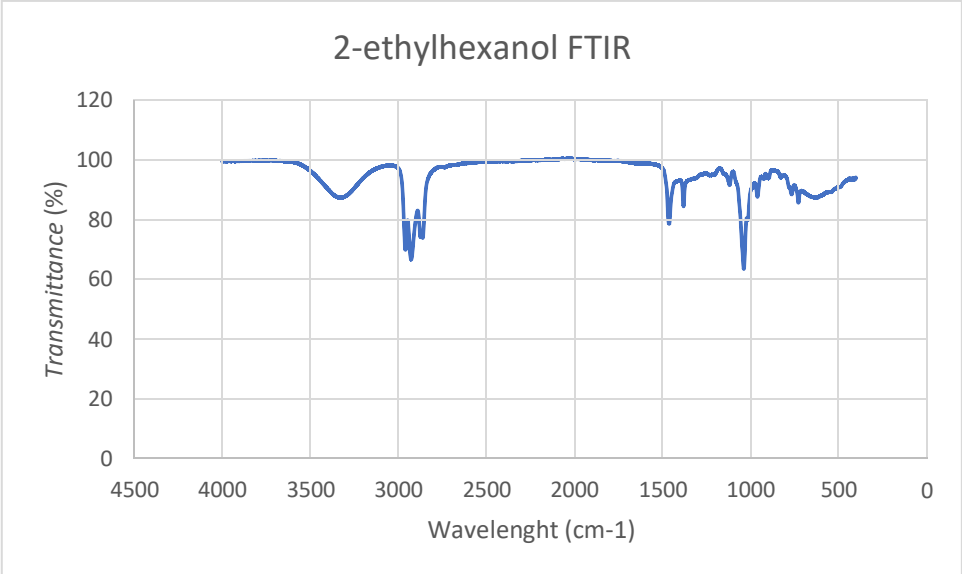

Figure 65 - 2-ethylhexanol FTIR

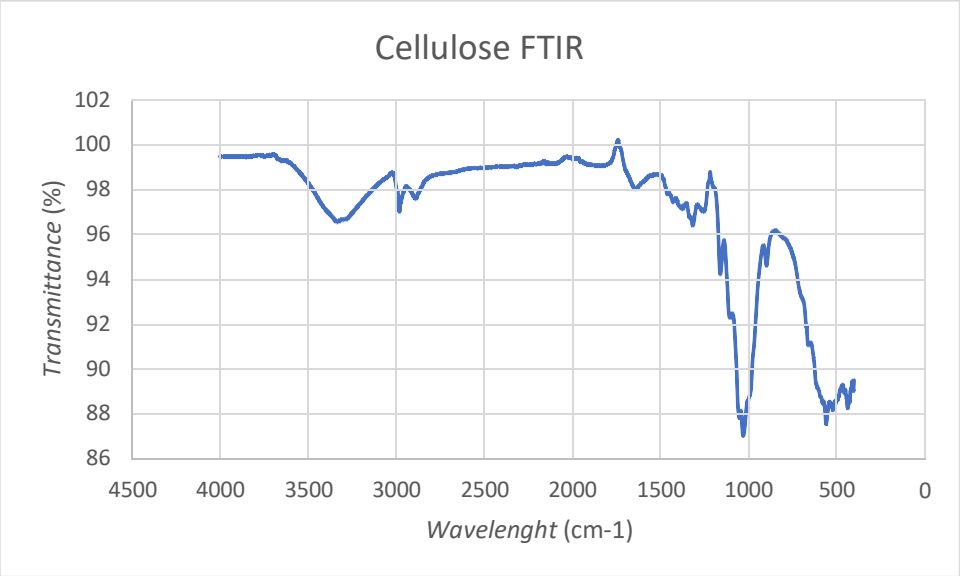

Figure 66 - Cellulose FTIR

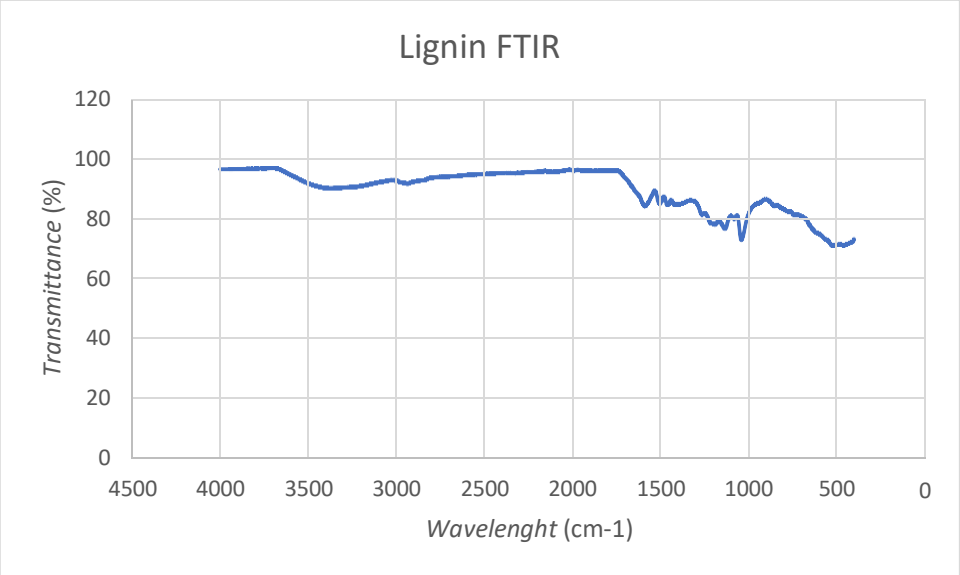

Figure 67 - Commercial Lignin FTIR